Arnold Schwarzenegger
Governor

COOL-COLOR ROOFING MATERIAL ATTACHMENT 8: TASK 2.6.2 REPORTS - MATERIALS TESTING AT WEATHERING FARMS IN CALIFORNIA

PIER FINAL PROJECT REPORT

Prepared For:
California Energy Commission
Public Interest Energy Research Program

Prepared By:
Lawrence Berkeley National Laboratory and Oak Ridge National Laboratory

ERNEST ORLANDO LAWRENCE
BERKELEY NATIONAL LABORATORY

June 2006
CEC-500-2006-067-AT8

Prepared By:
Lawrence Berkeley National Laboratory
Hashem Akbari
Berkeley, California
Contract No. 500-01-021

Oak Ridge National Laboratory
William Miller
Oak Ridge, Tennessee

Prepared For:
California Energy Commission
Public Interest Energy Research (PIER) Program

Chris Scruton
Contract Manager

Ann Peterson
Building End-Use Energy Efficiency Team Leader

Nancy Jenkins
PIER Energy Efficiency Research Office Manager

Martha Krebs, Ph.D.
Deputy Director
ENERGY RESEARCH AND DEVELOPMENT DIVISION

B. B. Blevins
Executive Director

Composition and Effects of Atmospheric Particles on the Performance of Steep-Slope Roofing Materials

Meng-Dawn Cheng* and William A. Miller
Oak Ridge National Laboratory
PO Box 2008
Oak Ridge, TN 37831

and

Paul Berdahl and Hashem Akbari
Lawrence Berkeley National Laboratory
Berkeley, CA 94720

Susan Pfiffner
University of Tennessee, Center for Biomarker Analysis, Knoxville, TN 37916

ABSTRACT

Novel cool color pigments have been developed that are dark in color but weakly absorbing and sometimes strongly scattering in the near infrared portion of the solar spectrum. The high near infrared reflectance of coatings colored with these "cool" pigments is being exploited to manufacture roofing materials that reflect more sunlight than conventional roofing products. The cool pigments result in lower roof surface temperature, which in turn reduces the building's cooling-energy demand. However, determining how weathering affects the solar reflectance and thermal emittance of cool pigmented roofs is of paramount importance for proving sustained thermal performance and thereby accelerating their market penetration in both residential and commercial applications.

Airborne particulate matter that settles on a roof can either reflect or absorb incoming solar radiation, dependent on the chemical content and size of the particles. These light scattering and absorption processes occur within a few microns of the surface, and can affect the solar reflectance of the roof. The long-term change in reflectance appears driven by the ability of the particulate matter to cling to the roof and resist being washed off by wind and or rain. Contaminants collected from samples of roof products exposed at seven California weathering sites were analyzed for elements and types of carbon to characterize the chemical profile of the particles soiling each roof sample and to identify those elements that degrade or enhance solar reflectance. The chemical composition of particles deposited on the roof samples was very similar across California; there was no clear distinction from one region to another. Organic and elemental carbon was detected; however, the amount of elemental carbon was too small to contribute significantly to the loss of solar reflectance. Dust particles (characterized by Ca and Fe) and organic carbon caused a loss of solar reflectance of highly reflective substrates and an increase in reflectance of dark materials.

INTRODUCTION

The long-term benefits of cool pigmented roofing systems (Akbari et al. 2004) can be compromised if a significant loss in solar reflectance occurs during the first few years of service life. Ultraviolet radiation, atmospheric pollution, microbial growths, acid rain, temperature cycling caused by sunlight and sudden thunderstorms, moisture penetration, condensation, wind, hail, and freezing and thawing are all thought to contribute to the loss of a roof's solar

reflectance. Wilkes et al. (2000) completed the testing of 24 different roof coatings on a low-slope test stand and observed about a 25% decrease[1] in the solar reflectance of white-coated and aluminum-coated surfaces as the time of exposure increased; however, the decrease leveled off after 2 years. SPRI Inc. and its affiliates studied the effect of climatic exposure on the surface properties of white thermoplastic single-ply membranes and determined that membranes lose from 30 to 50% of their reflectance over 3 years (Miller et al. 2002). The CMRC and its affiliates AISI, NamZAC, MBMA, MCA and NCCA exposed unpainted and painted metal roofing on both steep- and low-slope test roofs and found that after 3½ years, the painted polyvinylidene fluoride (PVDF) metal roofs lost less than 5% of their original reflectance (Miller et al. 2004). The results of the three different weathering studies are very interesting in terms of their solar reflectance after 3½ years of exposure. The white thermoplastic membrane and white ceramic coating with white topcoat had original reflectance measures that were about 20 percentage points higher than the painted metal; however, after 3-years of field exposure the solar reflectance of the painted metal exceeds that of the thermoplastic membrane and equals that of the coating.

Miller et al. (2002) discovered that aerosol deposition introduced biomass of complex microbial consortia onto the test roofs and the combination of contaminants and biomass accelerated the loss of solar reflectance for the thermoplastic membranes and the roof coatings. Airborne contaminants and biomass were also detected on the painted metal roofs; however, as stated the loss of solar reflectance was less than 5% for the painted metal roofs (Fig. 1). The chemistry of the PVDF paint resin system uses similar organic film bonding to that responsible for Teflon®, making it extremely chemical resistant and dirt shedding. Miller and Rudolph (2003) found the PVDF painted metals maintained solar reflectance even after 30 years of climatic exposure. Therefore the reduction of roof reflectance is closely related to the composition of the roof and to the chemical profile of the contaminants soiling the roof. Field data suggests that the loss of reflectance is due to dust load and or biomass accumulation, which in turn is affected by the climatic conditions. Biomass may be due to the growth of fungi and/or mold species that were transported by airborne particulate matter blown by the wind. Deposition of atmospheric carbon, nitrogen, and moisture accumulation on the roof provide suitable conditions for the colonization of these microbes.

Results published by Berdahl et al. (2002) indicate that the "the long-term change of solar reflectance appears to be determined by the ability of deposited soot to adhere to the roof, resisting washout by rain." Samples studied were bare metal and PVC roofing weathered for 18 years. Berdahl attributed soot, black carbon, and/or elemental carbon to be the primary cause of long-term reflectance loss. However, atmospheric particles are a class of complex mixtures consisting of directly emitted particles such as dusts from road traffics and particles from utility power plant emissions, and indirectly produced particles such as smog that are formed in the atmosphere through photochemical reactions. Deposition of any or all of these particles could cause changes in roof reflectance in addition to soot particles.

A reduction in solar reflectance of a substrate generally requires the presence of light absorbing particles. While soot containing elemental carbon (EC) is an important broadband absorber, two other potentially important absorbers are organic carbon (OC) and iron-containing minerals such as hematite. Organic carbon consists of hydrocarbon substances from combustion, carbon in the form of biomass, and possibly other substances. It is expected to absorb mainly in the short wave part of the visible spectrum (400 - 550 nm) (Kirchstetter et al., 2004). It also

[1] Percentage drops are based on fractional reductions by the formula: $100. * \left(\rho_{initial} - \rho_{aged}\right) / \rho_{initial}$

absorbs in the ultraviolet (UV) range but usually would not reduce the UV reflectance because the typical substrate is also UV absorbing. Hematite also absorbs in the short wave part of the visible range. Thus, hematite rust is reddish in color, due to non-absorbed red light. The details of the hematite absorption (Levinson et al., 2005) are, however, different from OC. It also absorbs in a band in the near infrared (800-900 nm).

An increase in solar reflectance requires the addition of light-scattering particles. For example, a white powder increases the reflectance of a black or gray substrate. The ability of a particle to scatter light is proportional to $(n_{pl}-n_o)^2$, where n_{pl} is the real refractive index of the particle and n_o is the refractive index of the surrounding medium. Many minerals and organic substances have refractive indices in the range of [1.3, 1.8] and therefore in air ($n_o = 1$) cause light scattering. Hematite has quite a high refractive index (~3, Wong and Brus, 2001) and therefore can contribute strongly to light scattering at wavelengths greater than 550 nm.

Suppose a substrate has a clean reflectance denoted R_o, which is coated with a thin soil layer with absorptance a and reflectance r. In view of the assumption that the layer is thin, we take both a and r as small compared to unity. Then, it is not difficult to show that the change in reflectance R of the soiled substrate is given, to first order in r and a, by $R - R_o = -2\,R_o\,a + (1-R_o)^2\,r$. Thus soil absorptance reduces R and soil reflectance increases R. Here we can also see that a will be less important if R_o is small and r will be less important if R_o is close to unity. Anticipating the data to come, we can hypothesize that highly reflective materials tend to lose their reflectance as they are soiled, with the reflectance loss determined by absorption of the soil. Very dark materials tend to become lighter as they are soiled, with the reflectance increase caused by light scattering by soil. It is plausible that the aged solar reflectance of roofs is affected by many factors including atmospheric deposition of soot particles and dusts (e.g., dirt, road dust, and soil particles). To study the issues further, characterization of the chemical and physical attributes of the deposited particles was conducted in the diverse climates of California.

Southern California is densely populated and known for its high volume of almost continuous traffic and emissions. The region is generally low in humidity with certain regions like El Centro having less than 3-in of annual precipitation, therefore making the area an excellent site for studying solar reflectance loss due to dusts and soot. Sufficient moisture is a major environmental condition needed for the growth of microbes such as mold and fungi, which can potentially reduce light reflectance. Under a dry climate, the microbial factor is lessened enabling the field study to focus more on the impacts of physical and chemical factors of aerosols.

The objectives of this study are (1) document the drop in solar reflectance and the change in thermal emittance for roof products having cool color pigments, (2) characterize the particulate matter deposited on roof samples of different materials, (3) establish the relationship between the deposited particulate matter and reduction of solar reflectance, and (4) quantify the contributions of the chemical composition of the particulate matter on the enhancement or loss of solar reflectance on a roof material.

WEATHERING SITES IN CALIFORNIA

Seven sites were selected for exposing painted metal, clay and concrete tile roof products with and without cool color pigments in the diverse climates of California (Table 1). Custom-Bilt Metal, Steelscape, BASF, MonierLifetile, US Tile, Maruhachi Ceramics of America, the Shepherd Color Company, American Rooftile Coatings and Elk Corporation supported the initiative by either field testing roof samples at their respective manufacturing facilities (Table 1) and/or by providing roof products for natural exposure testing. The California population is

expanding rapidly in the Central Valley and around the LA basin, and the sites with Custom-Bilt (Sacramento) and Elk (Shafter) capture the effects of weather, urban pollution and the expanding population. These areas reflect a market with many new homes. Weathering sites with Steelscape, BASF and Maruhachi Ceramics of America are located in existing densely populated areas of San Francisco basin and LA, and represent the market for re-roofing existing homes. Samples were also exposed near weather stations maintained by the California Irrigation Management Information System (CIMIS). Sites in McArthur and El Centro, CA. were selected for acquiring exposure data in the more extreme climates. McArthur is located in the moderate alpine climate of northern California (climate zone 16); El Centro is in the extremely hot desert climate of southern California bordering the Arizona state line (climate zone 15).

The CIMIS web site http://www.cimis.water.ca.gov/ has current weather data that can help estimate through regression analysis the loss of solar reflectance as affected by the climatic elements. In fact, CIMIS has 118 computerized weather stations acquiring hourly, daily, weekly and/or monthly solar irradiance, ambient air temperature and relative humidity as well as wind speed, wind direction and precipitation; Table 2 locates each weathering site and provides the closest CIMIS station to each weathering site. Solar reflectance (SR) of the new and aged samples is also provided for the different samples used for elemental contaminant and also for biomass determinations.

Exposure Racks

All roof samples were installed in exposure rack assemblies, which are 5.5-ft high by 9-ft long, and divided into three sub-frames having respective slopes of 2-, 4- and 8-in of rise for 12-in of run (i.e., slopes of 9.5°, 18.4° and 33.7°). Each sub-frame can hold two "Sure-Grip" sub-assemblies, which are designed to have 6 rows of samples with 34-in of usable space in each row. Sample size is 3.5-in by 3.5-in, a size that LBNL's Perkin-Elmer Lambda 900 spectrophotometer can easily accommodate for measuring the solar reflectance at discrete wavelengths. Finally all exposure rack assemblies were oriented facing south for full exposure to natural sunlight and weathering (Fig. 2).

Table 1. Weathering Sites for exposing roof products with and without cool color pigments.

Company	Contact	City	County	Climate Zone	Roof or Ground Mount
Department of Water Resources CIMIS	Sergio Fierro	El Centro (RS01)	Imperial	15	Ground
Maruhachi Ceramics of America	Yoshihiro Suzuki	Corona (RS02)	Riverside	10	Ground
BASF	Michelle Vondran	Colton (RS03)	San Bernadino	10	Roof
ELK Corporation	Gus Freshwater	Shafter (RS04)	Kern	13	Ground
Steelscape	Bruce Hopkins	Richmond (RS05)	Contra Costa	3	Roof
Custom-Bilt	Dan Bonnington	Sacramento (RS06)	Sacramento	12	Roof
Department of Water Resources CIMIS	Jamie Dubay	McArthur (RS07)	Shasta	16	Ground

Table 2. Identification of Coupons, location nearest CIMIS Station and solar reflectance data..

	El Centro (RS01)	Corona (RS02)	Colton (RS03)	Shafter (RS04)	Richmond (RS05)	Sacramento (RS06)	McArthur (RS07)
CIMIS Site[1]	87	44	44	5	157	131 & 155	43
Latitude	32°48'24"N	33°57'54"N	33°57'54"N	35°31'59"N	37°59'30"N	38°35'58"N	41°03'53"N
Longitude	115°26'46"W	117°20'08"W	117°20'08"W	119°16'52"W	122°28'12"W	121°32'25"W	121°27'16"W
Samples for Element Study	Gray Artic concrete tile	Gray Artic concrete tile	PVDF Metal Charcoal Gray	PVDF Metal Rawhide	PVDF Metal Rawhide	Gray Artic concrete tile	PVDF Metal Rawhide
Sample ID	976	676	517,518,519	704, 705, 706, 707	404,406	378	805,806
Sample Area (m^2)	7.903E-03	7.903E-03	2.371E-02	3.161E-02	1.581E-02	7.903E-03	1.581E-02
SR initial	0.27	0.25	0.31	0.57	0.57	0.27	0.57
SR after 1.63 yrs	0.28	0.23	0.30	0.52	0.55	0.25	0.55
Samples for Biomass Study	PVDF Metal Hartford Green	PVDF Metal Charcoal Gray	Gray Artic concrete tile	Buff Blend Clay tile	PVDF Metal Rawhide	Brown Artic concrete tile	PVDF Metal Rawhide
Sample ID	920, 921, 922, 923	616	576	779,780	405	372	804,807
Sample Area (m^2)	3.161E-02	7.903E-03	7.903E-03	1.581E-02	7.903E-03	7.903E-03	1.581E-02
SR initial	0.27	0.31	0.25	0.53	0.57	0.26	0.57
SR after 1.63 yrs	0.28	0.30	0.24	0.48	0.54	0.25	0.55
	[1] http://wwwcimis.water.ca.gov/cimis/welcome.jsp						

Solar Reflectance (SR) and Thermal Emittance (TE) Instruments

A Device and Services solar spectrum reflectometer was used to measure the solar reflectance (total hemispherical reflectance over spectrum of sun's energy) of the roof samples. The device uses a tungsten halogen lamp to diffusely illuminate a sample. Four detectors, each fitted with differently colored filters, measure the reflected light in different wavelength ranges. The four signals are weighted in appropriate proportions to yield the total hemispherical reflectance. The device was proven accurate to within ±0.003 units (Petrie et al. 2000) through validation against the ASTM E-903 method (ASTM 1996). However, because the CRCMs exhibit high infrared reflectance, some of the field samples were also measured at LBNL using a spectrometer to check the portable reflectometer. The average absolute difference between the Device and Services reflectometer and the spectrometer was about 0.02 points of reflectance with the spectrometer consistently reading lower than the reflectometer (as example, the reflectometer measured a solar reflectance of 0.741 for a IR painted metal while the spectrometer measured 0.73).

The impact of emittance on roof temperature is as important as that of reflectance. A portable Device and Services emissometer was used to measure the thermal emittance using the procedures in ASTM C-1371 (ASTM 1997). The device has a thermopile radiation detector, which is heated to 82.2°C (180°F). The detector has two high-ε and two low-ε elements and is designed to respond only to radiation heat transfer between itself and the sample. Because the device is comparative between the high-ε and the low-ε elements, it must be calibrated in situ using two standards, one having an emittance of 0.89, the other having an emittance of 0.06. Kollie, Weaver, and McElroy (1990) verified the instrument's precision as ±0.008 units and its accuracy as ±0.014 units in controlled laboratory conditions.

SOLAR REFLECTANCE AND THERMAL EMITTANCE

The solar reflectance and the thermal emittance of a roof surface are important surface properties affecting the temperature of a roof which, in turn, drives the heat flow across the roof. Akbari and Konopacki (1998) and Miller et al. (2004) showed that in moderate to predominantly hot climates, an exterior roof surface with a high solar reflectance and high infrared emittance will reduce the exterior temperature and produce savings in comfort cooling. For predominantly heating-load climates, surfaces with moderate reflectance but low infrared emittance save in comfort heating. Determining the affects of climatic soiling on the solar reflectance and infrared emittance of cool color roofs is therefore very important for developing realistic claims of the net energy savings (cooling energy savings less heating penalty).

Coupons of concrete and clay tile and painted metal roof samples were exposed to the elements in six of California's sixteen climate zones. The tabulation of the solar reflectance data for the seven weathering sites is provided in Appendix A. Contaminant samples were collected after 1.6 years of exposure for the coupons identified in Table 2, and the measures of solar reflectance and thermal emittance are reported herein for the Table 2 coupons to view the time dependence of climatic soiling and later, in the contaminants section, the impact of the various contaminants on the loss of solar reflectance.

Affects of Soiling on Solar Reflectance and Thermal Emittance

The painted PVDF coupon having an off-white color (Rawhide) steadily lost solar reflectance over the first year of exposure (Fig. 3). The loss varied from site to site with the least drop observed at McArthur (4%[1] after one year) and the worst occurring in the more desert-like areas of Shafter and Colton (23% after one year). The exposure rack in Colton is roof-mounted while the one in Shafter is ground mounted (Table 1), yet the change in solar reflectance after one year of exposure is very similar between the two sites. Inspection of the off-white painted metal coupon installed in the medium slope rack (4-in rise per 12-in run) at Shafter showed that after one year of exposure the sample was soiled with airborne debris (Fig. 4). However, after an additional 8 months of weathering the samples at all sites regained most of their solar reflectance (average SR loss of only 6% from starting SR value). El Centro and Shafter had less than ½–in of rainfall from Aug 04 through April 05; however, McArthur, Corona, Colton, Sacramento and Richmond had two consecutive months in early 2005 with rains exceeding 5-in per month. The average winds remained steady at about 4 to 5 mph over the entire exposure period at all sites. Hence the results are showing that the loss of reflectance is remedied in part by the combination of precipitation and wind sweeping or simply wind sweeping in the drier climates of El Centro and Shafter.

The darker charcoal gray coupon did not show the same seasonal variations in solar reflectance as the lighter coupon because its solar reflectance is roughly half that of the off-white painted metal (Fig. 5). Dusts tend to lighten darker colors and the soiling of the charcoal gray coupon slightly increased solar reflectance. Coupons of the same color but having conventional pigments (labeled standard in Fig. 3 and 5) have lower solar reflectance than do the cool pigmented colors during the entire exposure period. The result is important because climatic soiling did not cause the cool pigmented colors to degrade more than that observed for the conventional pigmented colors. Therefore the cool pigmented painted metals performed as well as their counterparts. Further, the infrared reflective pigments boost the solar reflectance of a dark more aesthetically pleasing color to about 0.3 to 0.4 (view standard versus cool pigments at start of exposure Fig. 5) and results for the charcoal gray painted metal shows only about a 3% drop in solar reflectance over about 1.6 years of exposure.

Similar findings were observed for the clay and concrete tile coupons (Fig. 6). The coupon had cool pigments added to a glaze coating applied atop the concrete. Results showed that both concrete and clay coupons lost less than 5% of their original solar reflectance (Appendix A). Finally, the effect of roof slope becomes somewhat significant for coupons exceeding an initial solar reflectance of 0.50, as observed for the off-white painted metal coupons displayed in Fig. 7. As stated the coupons collect dust with the worst soiling occurring for samples exposed in Colton (Fig. 7). The crisp and clear alpine climate of McArthur continues to show the lowest loss of reflectance (Fig. 7). Samples at Colton have the greatest amounts of soiling, and show that the drop in solar reflectance diminishes slightly as roof slope increases. However, neither El Centro nor McArthur show this trend with roof slope. Also the darker more aesthetically pleasing roof colors do not show the trend (Fig. 8). The darker charcoal gray coupon shows slight increases in solar reflectance with time in El Centro and in Colton because of the accumulation of dusts that tend to lighten a darker color (Fig. 8). The dusting effect is most evident on the conventional pigmented coupons (Fig. 8). Therefore the effect of roof slope appears more academic and its affect is secondary as compared to the soiling by airborne dust debris. It is also important to again point out that the cool pigmented colors maintain their solar reflectance as well as their conventional pigmented counterparts.

The thermal emittance of the painted metal, clay and concrete tile coupons has not changed much after 1.6 years of exposure in California (Table 3). Miller et al. (2004) and Wilkes et al. (2000) both observed little variation in the thermal emittance of painted and or coated surfaces. Consistent with reported findings, the thermal emittance did not vary from site-to-site nor did it change with time for these painted products. Thermal emittance of metals is strongly dependent on surface properties. Unpainted metals will over time oxidize; the metal oxide surface layer increases the thermal emittance (Miller and Kriner 2001). However, the paint finishes applied to PVDF metal and clay and concrete tile are very durable and there is therefore no adverse weathering effects observed for the thermal emittance of painted roof products.

Table 3. Thermal Emittance measured for roof coupons at different sites over time of exposure.

Roof Sample	Site	Thermal Emittance at Exposure Times (yrs)				
		0.000	0.748	0.962	1.630	2.493
Charcoal Gray PVDF Metal	Corona	0.83			0.82	0.84
	Richmond	0.82	0.82	0.82		
Rawhide PVDF Metal	Corona	0.86			0.84	0.87
	Richmond	0.83	0.84	0.84		
Apricot Buff Clay Tile	Corona					
	Richmond	0.86	0.83	0.83		
Gray Artic Concrete Tile	Corona		0.84			
	Richmond		0.84	0.84		

CONTAMINANTS STUDY

The contaminant study encompassed the identification of elements and carbons for characterizing the chemical profile of the particles soiling each roof sample. The study also included the identification of microbial consortia that might also soil the coupons and degrade the solar reflectance. The procedures used to detect and identify contaminants are reviewed to document the handling of samples and the analysis techniques used to identify particulates.

Procedure for Elemental Contaminants

Contaminants were swabbed from the concrete and painted metal coupons identified in Table 2. The coupons were exposed for about 1.63 years prior to collecting the contaminant samples. Figure 9 shows a cement sample, and three metal samples. The samples from a single site were removed from the exposure racks, wrapped in aluminum foil, stored in a zip plug bag and sent airfreight back to ORNL.

A standard operating procedure was developed for removing the deposited particulate materials from the roof samples. Each sample was placed in a laboratory sonicating[2] bath filled with 800 ml of distilled water held at room temperature (Fig. 10a). After 20 minutes, the sample was removed from the bath using sterilized stainless steel forceps. The water suspension was then poured into a filtration apparatus (shown in Fig. 10b) and vacuum applied to filter the suspended particulate onto the filters. The solution was divided into two 400-mL aliquots. One 400-mL sub-sample was filtered through a 47-mm diameter nylon filter (OSMONIC, Inc., 0.1µm pore size) that was subsequently analyzed for selected metal composition by a certified analytical lab at the Y12 facilities in Oak Ridge, Tennessee. The other 400-mL sub-sample was passed through the same filtration apparatus (Fig. 10b) through a 47-mm diameter glass fiber filter (Whatman 934-GF). About 100 mL of additional deionized water was used to rinse off any particulate matter (PM) that remained on the samples. However, very little was found visually in the rinsed portion indicating the sonicating task was reasonably thorough in the removal of the deposited PM. All the filters were placed in a laboratory dedicator and held overnight at room temperature before being analyzed. As quality control, 400 ml of deionized water was filtered through a nylon filter to create an analytical blank for metal species. A glass fiber blank was created similarly for carbon analysis. The filtration apparatus was rinsed three times using deionized water in between different filtration runs.

Inductively Coupled Plasma (ICP) – Atomic Emission Spectrometry (AES) was used for the analysis by the Y12 lab. The EPA 6010 protocol for filter analysis was followed for analysis of metal content on the filters. We chose to detect the following elements: aluminum, antimony, arsenic, barium, beryllium, boron, cadmium, calcium, chromium, cobalt, copper, iron, lead, lithium, magnesium, manganese, molybdenum, nickel, niobium, phosphorus, potassium, selenium, silicon, silver, sodium, strontium, sulfur, thallium, thorium, titanium, uranium, vanadium, zinc, and zirconium. Most of the elements were below the method's detection limits, indicating their absence in the deposited PM, and are not reported. For those reported, their concentrations are above the blank values which are above or equal to the detection limits. The carbon content was analyzed by a Sunset instrument (the Sunset Laboratory, Inc., Portland, OR) for total, elemental, and organic carbon. Three samples, each 1-square cm, were punched out from a 47-mm diameter quartz filter and analyzed by the instrument, and the average of the triplicate was assigned as the carbon concentration for the sample. If the coefficient of variation of the triplicate concentration is greater than ±5%, the sample is considered as non-uniform

[2] Sonicating agitates the bath using high-frequency sound waves.

deposition and the result may be discarded. In this study all the samples met the precision requirement and were retained in the subsequent data analysis. The Sunset instrument is capable of analyzing carbon content of a filter sample using the temperature and oxidation profiles of particulate carbonaceous species to define organic vs. elemental carbon (i.e., OC vs. EC). The total sum of OC and EC is called the total carbon of a sample.

Procedure for Biomass Detection

Another set of roof tiles and painted metals, separate from samples used in the contaminant study and weathered for 1.6 years in various locations in California, were shipped overnight for biomass analysis. Samples were swapped for lipid and quinone analyses and frozen at -80°C until extraction. Muffled glass fiber filters and sodium phosphate buffer were used to gently rub and retrieve depositional material from the roof samples. The recovered filters were extracted for microbial membrane lipids using a modified Bligh and Dyer extraction and subsequently fractionated into neutral, glyco and polar lipid classes (Bligh and Dyer, 1959; White et. al., 1979). Quinones, present in the neutral lipid fraction, were analyzed on the liquid chromatography-mass spectrometry (Geyer et. al., 2004). Polar lipid fraction was subjected to a sequential saponification/acid hydrolysis/esterification. The resulting PLFA methyl esters were separated, quantified and identified by gas chromatography-mass spectrometry (White and Ringelberg, 1998). Laboratory research was performed by Andrew Parsons (undergraduate), Amanda Smithgall, Maragret Gan and Susan Pfiffner at the University of Tennessee, Center for Biomarker Analysis (Parsons et al. 2005).

Fatty acid nomenclature is based on the fatty acid abbreviated by the number of carbon atoms (a), a colon, the number of unsaturated C-C bonds (b) followed by 'ω' followed by the number of carbons (c) from the methyl end of the molecule to the position of the unsaturation (e.g., a:bωc). For monoenoic fatty acids, the a:bωc molecule is followed by the suffix "c" for the cis- or "t" for trans-configuration. Branched fatty acids are described by iso (i) or anteiso (a), if the methyl branch is one or two carbons from the methyl end or by the position of the methyl group from the carboxylic end of the molecule. Quinones are designated as ubiquinones (UQ) and menaquinones (MK) with a number (4-14) which indicates the number of isoprene units. The PLFA results are presented as biomass in pmol/square cm or as cells/square cm using the conversion factor of 2.5 x 105 cells per pmol (Balkwill et. al. 1988). Community compositions are represented as mole percentage for individual PLFA or for PLFA structural groups. Structural groups are indicated as normal saturates (Nsat), terminally branched saturates (Tbsat), mid-chain branched saturates (Mbsat), monounsaturates (Mono), branched monounsaturates (Bmono), cyclopropyl fatty acids (Cyclo), and polyunsaturates (Poly).

CHEMICAL PROFILE OF ROOF PARTICULATES

Figures 11a-11g individually shows the concentration of each measured chemical species per sample area for the seven sites. At some sites only one sample was pulled, while at another site several samples were pulled just to obtain a sufficient quantity of contaminants (Table 2). All elements shown on the X-axis of each plot are those whose concentrations were higher than the method's detection limits and above the blank values.

Sulfur content in the roof samples was not large, which may be attributed to the absence of coal-fired power plants in California. Calcium is found to be in rather high abundance, except for the remote McArthur site in northeastern California. Due to the small amount of sulfur present, the calcium is likely to be in the form of carbonate (rather than sulfate). Aluminum (Al),

calcium (Ca), iron (Fe), manganese (Mn), and silicon (Si) are the elements consistently found at all seven sites. Potassium (K) was found high at RS02 (Corona), RS03 (Colton), and RS04 (Shafter) sites.

OC values are higher than EC values for all sites. The McArthur site that is located in an alpine climate rather than the industrial and or urban environments of the other sites had the least amount of EC per unit area of pulled sample. Plants and vegetations are excellent sources of emission of organic compounds that could be detected as OC, if the compounds or their reaction products were found on particulate matter. On the other hand, elemental carbons (e.g., soot) emanate from combustion source emissions such as vehicle engine exhausts. We thus attributed the observed higher EC values in Shafter, Richmond and Sacramento to potential contributions by traffics and vehicle emissions at the sites. The traffic volume around the McArthur site area is much less than other areas because of its rural setting, but McArthur is in a forest area where biogenic emissions might be significant. This resulted in higher OC than EC, and the data reported here support this understanding.

To further study the sources of carbon content in aerosol particles, we computed the ratios of EC to OC for the seven sites based on the data shown in Figs 11a-11g. The EC/OC ratio has been successfully used by Appel et al., 1976, Turpin and Huntzicker, 1995, and Strader et al., 1999 to identify whether the carbon in aerosol was primary or secondary in content. If the EC/OC ratio is low and correlation between OC and EC is high, the carbon likely emanates from direct emissions. Average EC/OC value reported by Appel et al., 1976, Turpin and Huntzicker, 1995, and Strader et al., 1999 is about 0.48 in winter, 0.32 in spring, and 0.18 in summer. The EC/OC ratios computed for the seven sites were all smaller than 0.18, much smaller than 0.48. These results suggest, averaged over the 1.6 years, the carbon contents found on PM deposited at these sites were driven primarily by sources such as biogenic emissions and or forest or local brush fire rather than photochemical conversion.

Many of the metals analyzed for all sites are of crustal origins such as road dusts, soil, and or rock debris. The results presented in Fig 11a-11g indicate two major contributors of particulate matter: crustal sources and traffic activities. The importance of these two source categories and their impacts on the performance of roof samples in terms of loss of solar reflectance over time is addressed in the Section “Effect of particulate matter on solar reflectance of roof material”.

Cross correlation of the samples

The pair-wise Spearman rank correlation coefficients among the seven weathering sites were calculated using StatGraphics™ and tabulated in Table 4. The Spearman rank correlation is a nonparametric (distribution-free) rank statistic used as a measure of the strength of the associations between two variables; refer to Lehmann and D'Abrera (1998) for review of the formula used for calculating the Spearman rank correlation coefficient.

The rank correlation yielded coefficients all greater than 0.93 for El Centro, Corona, and Colton. These three sites are in the southern California, and the high ranking indicates particles of similar chemical composition were deposited at these 3 sites. This is reasonable considering that these three sites are in the same region or airshed. Composition of particles deposited at the Shafter site appears to correlate well with the northern and southern sites. The three northern California sites (McArthur, Sacramento, and Richmond), however, do not have strong correlation among themselves similar to the three southern sites. The coefficient for the

Table 4. Spearman Rank Correlation Coefficients for the Seven Sites Included in the Study

	El Centro	Corona	Colton	Shafter	Richmond	Sacramento	Macarthur
El Centro	1.00						
Corona	0.96	1.00					
Colton	0.93	0.97	1.00				
Shafter	0.86	0.92	0.85	1.00			
Richmond	0.92	0.91	0.91	0.83	1.00		
Sacramento	0.62	0.71	0.61	0.88	0.55	1.00	
McArthur	0.75	0.76	0.65	0.86	0.62	0.87	1.00

Sacramento-Richmond pair is 0.55, and the Richmond-McArthur is 0.62. Both values do not suggest strong similarity. The Sacramento-McArthur pair however has a coefficient of value 0.87 that is reasonably high. McArthur, being a rural site in northern California, only mildly correlates with the sites in southern California. The inland site in Sacramento only correlates well with Shafter, and shows statistically weak correlation with any southern sites and Richmond, which is located near the San Francisco bay area.

Effect of particulate matter on solar reflectance of roof materials

The time-integrated (over 1.6 years) solar reflectance measurement data from the seven sites were mapped onto the chemical profiles shown in Figs 11a-11g by a linear function in an attempt to determine important chemical elements that have contributed to the degradation of roof reflectance. The degradation of roof solar reflectance for each site was computed as the difference between the reflectance value measured at 1.6 years and at time zero. The linear function was defined by the formulation:

$$R_{(n,1)} = C_{(n,\,p)} w_{(p,1)} \qquad (1)$$

where

- R an n by 1 vector of time-integrated reduction of solar reflectance,
- n the number of sites,
- C chemical profiles of deposited particles obtained from the sites using an n by p matrix,
- p number of chemical species in a profile, and
- w weights for the chemical species in a p by 1 vector.

We selected a smaller set of elements containing the following 16 variables: Al, Ca, Cr, Cu, Fe, Mn, Mg, Ni, K, Si, Na, S, V, Zn, OC, and EC for solving Eq. (1) above. We eliminated a variable if the concentration for this variable was zero at each sampling site. We also removed those that we felt unlikely to give us any useful information based on our prior experience in atmospheric aerosol research (e.g., Cheng and Hopke, 1989). We estimated the contribution of each of the selected elements to the 1.6-year integrated solar reflectance reduction values by performing a least-square optimization operation (constrained to go through a zero intercept) in

which the objective is to minimize the square root of the differences between the observed and calculated reflectance values. Table 5 shows the result of the optimization.

Table 5. Least Squares Optimization showing regression coefficients for detected elements.

1	Al (Aluminum)	**-0.0010**	9	K (Potassium)	0.0003
2	Ca (Calcium)	0.0001	10	Si (Silicon)	0.0003
3	Cr (Chromium)	0.0000	11	Na (Sodium)	0.0000
4	Cu (Copper)	0.0000	12	S (Sulfur)	0.0000
5	Fe (Iron)	0.0004	13	V (Vanadium)	0.0000
6	Mn (Manganese)	0.0000	14	Zn (Zinc)	0.0006
7	Mg (Magnesium)	0.0000	15	OC (Organic Carbon)	**-0.0014**
8	Ni (Nickel)	0.0000	16	EC (Elemental Carbon)	0.0000

A positive value in Table 5 indicates the element might contribute to the reduction of solar reflectance, while a negative value indicates the opposite that the element could contribute to the increase of solar reflectance. Results shown in Table 5 indicate, statistically, Cr, Cu, Mn, Mg, Ni, Na, S, V, and EC have no contributions to the change of solar reflectance values. Al and OC contributed to the increase of solar reflectance values found at the sites, and Ca, Fe, K, Si, and Zn could contribute to the degradation of solar reflectance measured on the roof samples. Aluminum oxide has a refractive index of about 1.7, and its particles can thus bereflective in the visible to infrared region. Organic carbon, OC, is a highly complex mixture of materials containing carbon that can be detected in the form of CO_2 when burned. OC is well-known to be a reflective component of aerosol particles (see Novakov and Penner, 1993 in http://eetd.lbl.gov/newsletter/nl17/blackcarbon.html, for example) due to its ability to scatter light. OC absorbs at short wavelengths (UV and blue), but is reflective at longer wavelengths.EC is commonly referred to as black carbon or soot and is believed to be a significant factor in the loss of a roof's solar reflectance (Berdahl et al., 2002). Our regression result here does not indicate the significance of EC in contributing to the degradation of roof solar reflectance.

To obtain a semi-quantitative estimate of the maximum possible optical absorption of the iron, we assume that 70 mg/m^2 are present in the form of small (e.g., 0.27 μm diameter) hematite (Fe_2O_3) pigment particles (Levinson *et al*., 2005). Hematite is a strong absorber of the short wavelength part of the solar spectrum (300 to 550 nm) and a hematite layer could absorb a measurable portion (~28 %) of the short wavelength component. The reported Fe result does support the hypothesis on short-wavelength absorption. A more detailed analysis of solar absorption associated with iron is presented in Appendix B. The complex mixture of atmospheric particles is somewhat confounding the light extinction process as described by the simple linear model of chemical elements. It might be desirable to analyze the crystalline structure of all potential elements in future research.

Discussion of carbon effects on roof solar reflectance

The role of elemental carbon (i.e., soot) if in significant content in aerosols can be dramatic. Fig. 12 shows the expected solar reflectance and visible reflectance as a function of soot concentration, as a fraction of the initial high reflectance R_o (Berdahl et al., 2006). The OC and EC amounts measured in mg per unit area in meter squared at these seven sites are shown in Table 6. The largest EC per unit area was found at Richmond, while the blank filter had virtually no EC. Note that the detection limit for carbon is 0.2 μg. For the sample exposed at Richmond,

Table 6. Derived OC and EC Amounts per Unit Area on the Roof Samples Collected at the seven Sites (Detection Limit of Carbon is 0.2 µg)

Site ID	Organic Carbon (mg/m^2)	Elemental Carbon (mg/m^2)
Blank Filter	**0.257**	0.007
El Centro	8.312	0.237
Corona	5.361	0.240
Colton	6.146	0.165
Shafter	5.591	0.404
Richmond	11.090	1.344
Sacramento	4.461	0.221
McArthur	1.315	0.018

with the largest amount of EC, 1.34 mg per square meter, EC was found to have contributed only 2-3% degradation of its original reflectance. Most of the samples were not greatly affected in reflectance by EC or the soot (< 10%), and the sample from McArthur is virtually unsoiled by soot. In other words, EC was found in too small concentrations to be a significant contributor in reducing surface reflectance at all seven sites in California.

BIOMASS AND COMMUNITY COMPOSITION OF ROOF SAMPLES

Membrane lipids were investigated to gain a better understanding of the microbial community composition and biodensity deposited or residing on these roof samples in the different California environments. Phospholipid fatty acid methyl esters (PLFA) have been used as biomarkers of microbial communities for many years. PLFA analysis is a direct real time monitoring analysis for viable biodensity of microbial communities because they degrade rapidly upon cell death (White et al., 1979). All eukaryote and bacterial cell membranes have PLFA which provide a non-selective means to assay changes in microbial communities (Tunlid and White, 1992, Federle et al., 1986; Findlay and Dobbs, 1993). PLFA ratios may also provide insight on metabolic status and stress of a community (Kieft et al., 1994; Frostagärd et al. 1996). Numerous studies used PLFA analysis to aid in determining microbial community composition and the impact of environmental factors like contamination by hydrocarbons (Pfiffner et al. 1997; Stephens et al., 1998) or metals (Brandt et al. 1999; Bääth et al., 1998).

Biomass PLFA and Quinone

The viable biomass as represent by PLFA composition is shown in Figure 13a. When biomass is converted to cells based on factors described by Balkwill et al. (1988), clay tiles averaged 1.25×10^6 cells per square cm compared to 6.0 and 1.5×10^5 cells per square cm for concrete and metal respectively. We speculate that the biomass may correspond to the texture of the tiles (metals were smooth, while clay tiles were rough). An additional plot (Fig. 13b) shows the average PLFA biomass for each roof material. When comparing biomass estimates based on

quinone composition (Fig. 14a), we did not see a similar trend with the PLFA biomass (Figure 13b and 14b). This may be due to the fact that neutral lipids do not degrade as quickly as PLFA. We speculate that the overall biomass may relate to the material composition of the tiles, i.e. concrete is more alkaline and to surface roughness which may have provided more pockets for particle or bacterial accumulation.

When comparing biomass with solar reflectance, we found that solar reflectance at 1.6 yrs was weakly correlated to increased biomass (R^2=0.51), which is consistent with finding from the contaminant study which showed OC to increase reflectance.

Community Composition

When interpreting the PLFA profiles, 18:2ω6 was the most prominent PLFA ranging from 21-44 mol% (Figure 15). This PLFA is indicative of cyanobacteria and fungi (Weete, 1974). Other major PLFA were 16:0, 18:1ω9c, 18:1ω7c, 18:0 in decreasing relative abundance. The normal saturate PLFA, 16:0 and 18:0, are ubiquitous and are generally seen in all PLFA profiles whereas the 18:1's are indicative of Gram-negative bacteria (Findlay and Dobbs 1993). A15:0 and i16:0 were found in clay and concrete tile, while only clay tiles showed br17:0 and br18:0. These terminally and mid-chain branched saturates are generally found in Gram-positive bacteria. Stress PLFA indicator for Gram-negative bacteria, cy17:0, was seen in the alpine climate (Guckert et al., 1986).

Quinone composition may be used to assess respiratory potential of the microbial community (Geyer et al. 2004). When Gram-negative bacteria and eukaryotes are growing with oxygen, ubiquinones are produced. Under reduced oxygen conditions, Gram-negative and archaeal bacteria produce menaquinones. Gram-positive bacteria produce menaquinones under aerobic and anaerobic conditions. In the figure 16, the quinone profiles are shown. Concrete tiles and the PVDF metal from McArthur had no menaquinones, which suggest an aerobic environment and a lack of Gram-positive bacteria. Clay and PVDF metals from Corona and Meloland showed diverse quinones profiles, which suggest the potential for various microorganisms. Clay and PVDF metal sample from Meloland had UQ/MK ratio of 0.37 to 0.44 and may indicate the presence of microphilic to anaerobic niches.

CONCLUSIONS

Seven sites were selected for exposing painted PVDF metal, clay and concrete tile coupons with and without cool pigmented colors in the arid, alpine, urban populated and also the cool, humid climates of California. The loss in solar reflectance for painted metal and clay and concrete tile coupons was of the order 6% of the initial reflectance for this 2½ year time limited study. Solar reflectance of the cool pigmented coupons always exceeded that of the convention pigmented coupons. Climatic soiling did not cause the cool pigmented roof coupons to lose any more solar reflectance points than their conventional pigmented counterparts. The effect of roof slope appears to have more of an affect on lighter color roofs whose solar reflectance exceeds at least 0.5 and visual shows the accumulation of airborne contaminants. However, precipitation and or wind sweeping helps restore most of the initial solar reflectance. The thermal emittance remained invariant with time and location and was therefore not affected by climatic soiling.

The roof samples collected at seven California sites have been analyzed for elements and carbons by using ICP-AES and Sunset OC/EC instruments following certified analytical procedure. A particle extraction procedure was developed to obtain particles from the roof samples in a consistent manner. The chemical profile of the particles collected by each roof

sample was obtained and reported for the seven sites. Analysis of cross-correlation of the seven chemical profiles shows a clear separation between the rural and urban/industrial sites and correlation among sites in a region; e.g., Southern California. There was also a weak separation between the sites in northern and southern California. We also attempted to identify the elements that contribute to the loss or enhancement of solar reflectance by performing a least-square optimization of the data. The results showed elemental or black carbon did not contribute significantly to the degradation of reflectance, but dust particles (characterized by Al) and organic carbon had a statistically significant effect on balancing the degradation over the course of 1.6 years.

Differences in microbial communities and biomass were seen between the various tile types and climate zones. Abundance of microbial biomass on roof tiles appears to be related to the composition/surface structure of the tile. When examined by PLFA and quinone analyses, some tiles showed diverse microbial communities. Cyanobacteria or fungi represent the dominant player. Future research includes molecular analysis for community composition and phylogenetic identification is ongoing. DNA has been extracted and will be analyzed using selected kingdom gene probes for bacteria and eukaryotes and specific gene probes for cyanobacteria followed by denaturing gradient gel electrophoresis and sequencing of selected bands for phylogenetic identification.

ACKNOWLEDGEMENTS

Funding for this project was provided by the California Energy Commission's Public Interest Energy Research program through the U. S. Department of Energy under contract DE-AC03-76SF00098. The authors acknowledge Doh-Won Lee of Oak Ridge Associated Universities for assistance in analyzing the filter samples for carbon content. The elemental composition of particles was analyzed by the analytical chemistry services at the DOE Y12 complex using ICP-AES instrument. Oak Ridge National Laboratory is managed by UT-Battelle, LLC, for the U.S. Dept. of Energy under contract DE-AC05-00OR22725. The submitted manuscript has been authored by a contractor of the U.S. Government under contract DE-AC05-00OR22725. Accordingly, the U.S. Government retains a nonexclusive, royalty-free license to publish or reproduce the published form of this contribution, or allow others to do so, for U.S. Government purposes.

DISCLAIMERS

Mention of the trade names, instrument model and model number, and any commercial products in the manuscript does not represent the endorsement of the authors nor their employer, the Oak Ridge National Laboratory or the US Department of Energy.

NOMENCLATURE

CIMIS	California Irrigation Management Information System
CMRC	Cool Metal Roof Coalition
AISI	American Institute of Steel Industries
NamZac	Galvalume Sheet Producers of North America
MBMA	Metal Building Manufacturers Association
MCA	Metal Construction Association
NCCA	National Coil Coaters Association
PVC	polyvinylchloride thermoplastic membranes

SR	solar reflectance
TE	thermal emittance
PM	particulate matter
Nsat	terminally branched saturates
Tbsat	mid-chain branched saturates
Mbsat	monounsaturates
Mono	branched monounsaturates
Bmono	cyclopropyl fatty acids
Poly	polyunsaturates

REFERENCES

Akbari,H., P. Berdahl, R. Levinson, R. Wiel, A. Desjarlais, W. Miller, N. Jenkins, A. Rosenfeld, C. Scruton (2004) Cool Colored Materials for Roofs, *ACEEE Summer Study on Energy Efficiency in Buildings.* Proceedings of American Council for an Energy Efficient Economy, Asilomar Conference Center in Pacific Grove, CA, August.

Akbari, H., Konopacki, S.J. 1998. "The Impact of Reflectivity and Emissivity of Roofs on Building Cooling and Heating Energy Use," in Thermal Performance of the Exterior Envelopes of Buildings, VII, proceedings of ASHRAE THERM VIII, Clearwater, FL., Dec. 1998.

ASTM. 1997. Designation C 1371-97: Standard Test Method for Determination of Emittance of Materials Near Room Temperature Using Portable Emissometers. American Society for Testing and Materials, West Conshohocken, PA.

_____. 1996. Designation E903-96: Standard Test Method for Solar Absorption, Reflectance, and Transmittance of Materials Using Integrating Spheres. American Society for Testing and Materials, West Conshohocken, PA.

Appel, B. R., P. Colodny, and J. J. Wesolowski (1976) Analysis of Carbonaceous Materials in Southern California Atmospheric Aerosols, Environ. Sci. Technol., 10: 359-363,

Bååth E, Diaz-Ravina M, Frostegård Å, Campbell CD. 1998. Effect of metal-rich sludge amendments on the soil microbial community. Appl Environ Microbiol 64:238-245.

Balkwill DL, Leach FR, Wilson JT, McNabb JF, White DC. 1988. Equivalence of microbial biodensity measures based on membrane lipid and cell wall components, adenosine triphosphate, and direct counts in subsurface sediments. Microbial Ecol 16:73-84.

Berdahl, P., H. Akbari, and L. S. Rose (2002) Aging of Reflective Roofs: Soot Deposition, *Appl. Opt.*, April 2002 Vol. 41, No. 12, 2355-2360.

Berdahl, P., H. Akbari, R. Levinson, and W. A. Miller (2006) Weathering of Roofing Materials-An Overview, in preparation.

Bligh EG, Dyer WJ. 1959. A rapid method of total lipid extraction and purification. Can J Biochem Phys 37:911-917.

Brandt CC, Schryver JC, Pfiffner SM, Palumbo AV, Macnaughton S. 1999. Using artificial neural networks to assess changes in microbial communities. In: Leeson A, Alleman BC, editors. Bioremediation of Metals and Inorganic Compounds. Columbus: Battelle Press. pp. 1-6.

Cheng, M.-D. and P. K. Hopke (1989) Identification of Markers for Chemical Mass Balance Receptor Model, *Atmos. Environ.*, 23(6): 1,373.

Federle, T.W., Dobbins, D.C., Thornton-Manning, J.R. and Jones, D.D. (1986) Microbial biomass, activity, and community structure in subsurface soils. 24: 365-374.

Findlay RH, Dobbs FC. 1993. Quantitative description of microbial communities using lipid analysis. In: Kemp PF, Sherr BF, Sherr EB, Cole JJ editors. Handbook of Methods in Aquatic Microbial Ecology. Boca Raton, FL. Lewis Publishers. p 271-284.

Frostegård, Å, Tunlid, A, Bååth, E. 1996. Changes in microbial community structure during long-term incubation in two soils experimentally contaminated with metals. Soil Biol Biochem 28:55-63.

Geyer, R., A.D. Peacock, D.C. White, C. Lytle and G.J. Van Berkel. 2004. Atmospheric pressure chemical ionization and atmospheric pressure photoionization for simultaneous mass spectrometric analysis of microbial repiratory ubiquinones and menaquinones. J. Mass Spectrometry 39:922-929.

Guckert JB, Hood MA, White, DC. 1986. Phospholipid, ester-linked fatty acid profile changes during nutrient depletion of Vibrio cholerae: increases in the trans/cis and proportions of cyclopropyl fatty acids. Appl Environ Microbiol 52:794-801.

Kieft, TL, Ringelberg, DB, White, DC. 1994. Changes in ester-linked phospholipid fatty acid profiles of subsurface bacteria during starvation and desiccation in a porous medium. Appl Environ Microbiol 60:3292-3299.

Kirchstetter, T. W., T. Novakov, and P. V. Hobbs (2004) Evidence that the spectral dependence of light absorption by aerosols is affected by organic carbon, J. Geophysical Research-Atmospheres 109, (D21): Art. No. D21208.

Kollie, T. G., F.J. Weaver, D.L. McElroy. 1990. "Evaluation of a Commercial, Portable, Ambient- Temperature Emissometer." Rev. Sci. Instrum., Vol. 61, 1509–1517.

Lehmann, E. L. and D'Abrera, H. J. M. (1998) *Nonparametrics: Statistical Methods Based on Ranks, rev. ed.* Englewood Cliffs, NJ: Prentice-Hall, pp. 292, 300, and 323.

Levinson, R, P. Berdahl, and H. Akbari (2005) Solar spectral optical properties of pigments – part II: survey of common colorants, Sol. Energy Mater. Sol. Cells 89, 351-389 (2005), Fig. 1, Film R03.

Miller, W.A., A. Desjarlais, D.S. Parker and S. Kriner (2004) Cool Metal Roofing Tested for Energy Efficiency and Sustainability, Proceedings of CIB World Building Congress, Toronto, Ontario, May 1-7, 2004.

Miller, W.A., Cheng, M-D., Pfiffner, S., and Byars, N. (2002) *The Field Performance of High-Reflectance Single-Ply Membranes Exposed to Three Years of Weathering in Various U.S. Climates*, Final Report to SPRI, Inc., Aug., 2002.

Miller, W. and B. Rudolph (2003), *Exposure Testing of Painted PVDF Metal Roofing*, Report prepared for the Cool Metal Roof Coalition.

Miller, W. A., and Kriner, S. 2001. "The Thermal Performance of Painted and Unpainted Structural Standing Seam Metal Roofing Systems Exposed to One Year of Weathering," in Thermal Performance of the Exterior Envelopes of Buildings, VIII, proceedings of ASHRAE THERM VIII, Clearwater, FL., Dec. 2001.

Novakov, T. and Penner, J.E. (1993) Large Contribution of Organic Aerosols to Cloud-Condensation-Nuclei Concentrations, *Nature*, 365, 823- 826.

Parsons, A., A. Smithgall, M. Gan, W. Miller, C.D. Cheng, and S.M. Pfiffner. September 2005. Influence of Microbial Deposition on High-Reflectance Roof Tiles. Kentucky-Tennessee Branch of the American Society of Microbiology, Nashville, TN.

Petrie, T. W., A.O. Desjarlais, R.H. Robertson and D.S. Parker. 2000. Comparison of techniques for in-situ, non-damaging measurement of solar reflectance of low-slope roof membrane.

Presented at the 14th Symposium on Thermophysical Properties and under review for publication in International Journal of Thermophysics, Boulder, CO; National Institute of Standards and Technology.

Pfiffner SM, Palumbo, AV, Gibon T, Ringelberg DB, McCarthy JF. 1997. Relating groundwater and sediment chemistry to microbial characterization at BTEX-contaminated site. Appl Biochem Biotech 63-65:775-788.

Stephen JR, Chang Y-J, Gan YD, Peacock A, Pfiffner SM, Barcelona MJ, White DC, Macnaughton SJ. 1998. Microbial characterization of PJ-4 fuel contaminated site using a combined lipid biomarker/PCR-DGGE based approach. Enivron Microbiol 1:231-241.

Strader, R., P. Lurmann, and S. P. Pandis (1999) Evaluation of Secondary Organic Aerosol Formation in Winter, *Atmos. Environ*., 33: 4849-4863.

Tunlid, A, White, DC. 1992. Biochemical analysis of biomass, community structure, nutritional status and metabolic activity of the microbial community in soil. In: Bollag J-M, Stotzky G, editiors. Soil Biochemistry Vol. 7. –. New York: Marcel Dekker Inc., pp. 229-262.

Turprin, B. J. and J. J. Huntzicker (1995) Identification of Secondary Organic Aerosol Episodes and Quantitation of Primary and Secondary Organic Aerosol Concentrations during SCAQS, *Atmos. Environ*., 29: 3527-3544.

Weete JD. 1974. Fungal Lipid Biochemistry: Distribution and Metabolism. New York: Plenum Press.

White DC, Davis WM, Nickels JS, King JD, Bobbie RJ. 1979. Determination of the sedimentary microbial biodensity by extractable lipid phosphate. Oecologia 40: 51-62.

White DC, Ringelberg DB. 1998. Signature Lipid Biomarker Analysis. In Techniques in Microbial Ecology. R. S. Burlage, R. Atlas, D. Stahl, G. Geesey, and G. Sayler, editors. Oxford University Press, New York, NY., pp. 255-272.

Wilkes, K. E., Petrie, T. W., Atchley, J. A., and Childs, P. W. (2000) Roof Heating and Cooling Loads in Various Climates for the Range of Solar Reflectances and Infrared Emittances Observed for Weathered Coatings, pp. 3.361-3.372, *Proceedings, 2000 Summer Study on Energy Efficiency in Buildings.* Washington, D.C.: American Council for an Energy-Efficient Economy.

Wong, S. S. and L. E. Brus (2001) Narrow Mie Optical Cavity Resonances from Individual 100 nm Hematite Crystallites, J. Phys. Chem. B 105, 599-603.

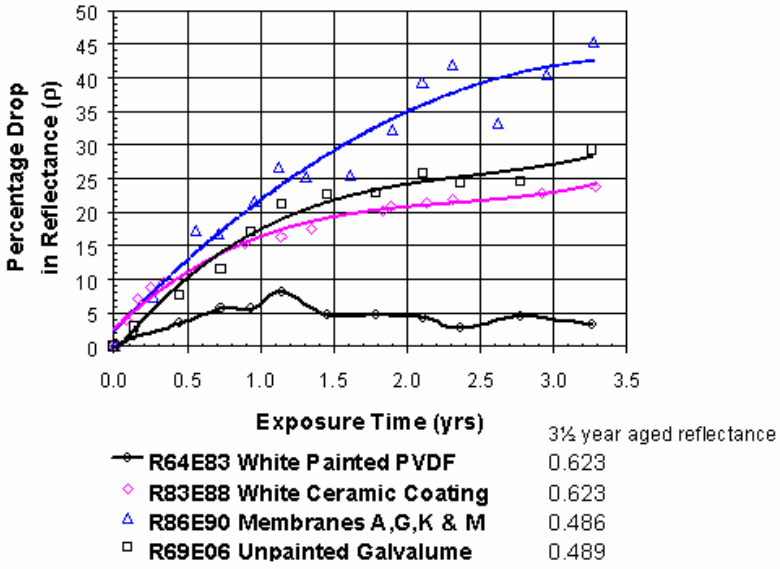

Fig. 1. Loss of solar reflectance for thermoplastic membrane, white ceramic coating and painted PVDF metal and bare Galvalume® roofs after three years of exposure.

Fig. 2. Exposure Rack Assembly used for natural exposure roof samples in seven California climatic zones; site shown is the Elk Manufacturing facility in Shafter, CA.

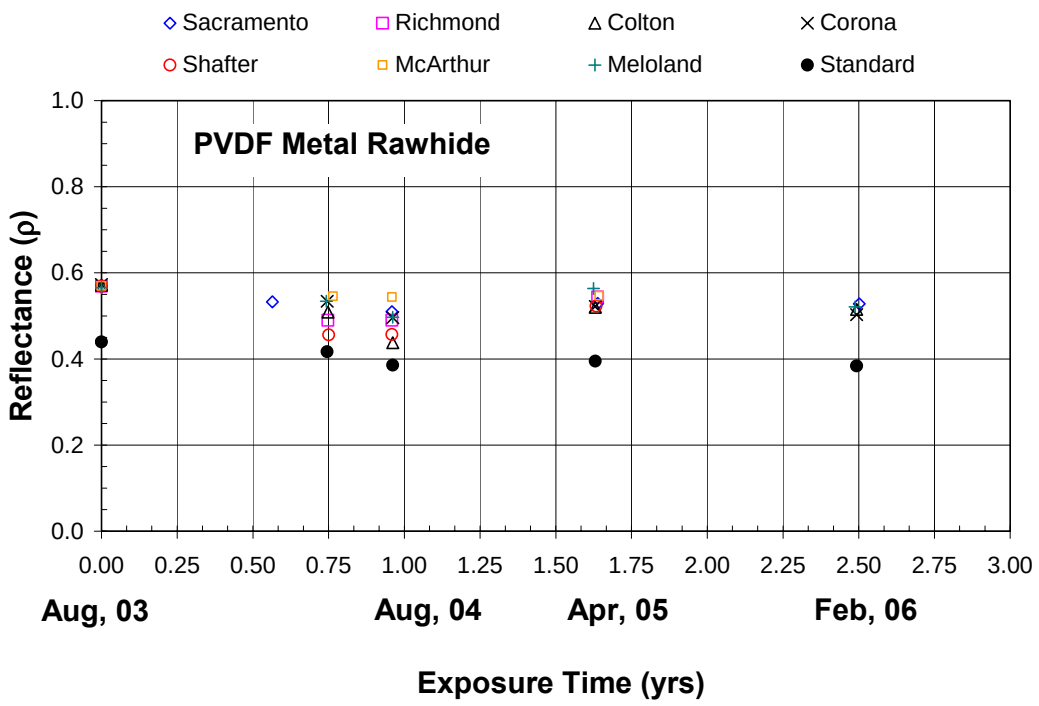

Fig. 3. Solar reflectance of a painted PVDF metal coupon (off-white color) at the seven CA weathering sites.

Fig. 4. Painted PVDF metal coupon soiled at the Shafter site after 1 full year of exposure.

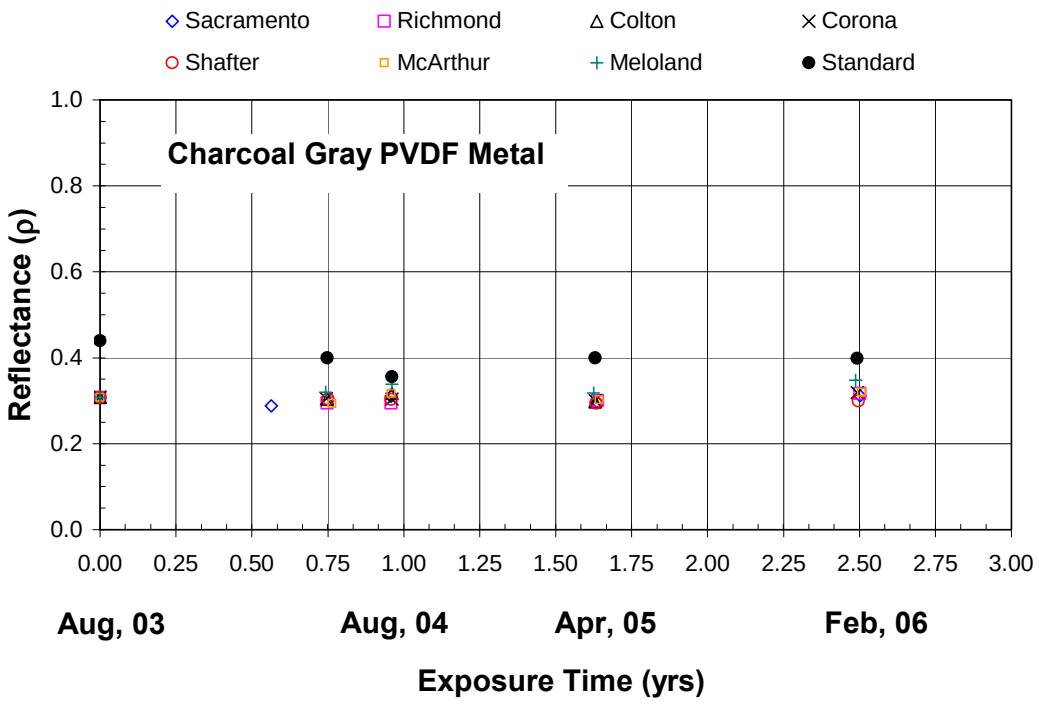

Fig. 5. Solar reflectance of a painted PVDF metal coupon (charcoal gray color) at the seven CA weathering sites.

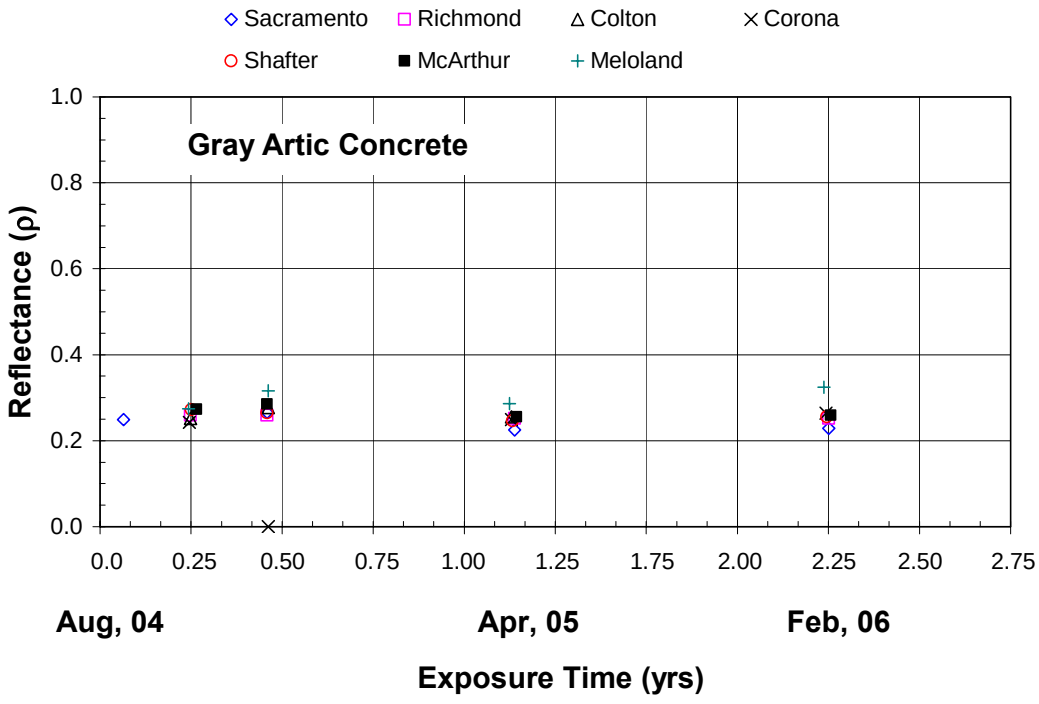

Fig. 6. Solar reflectance of a concrete tile coupon (light gray color) at the seven CA sites.

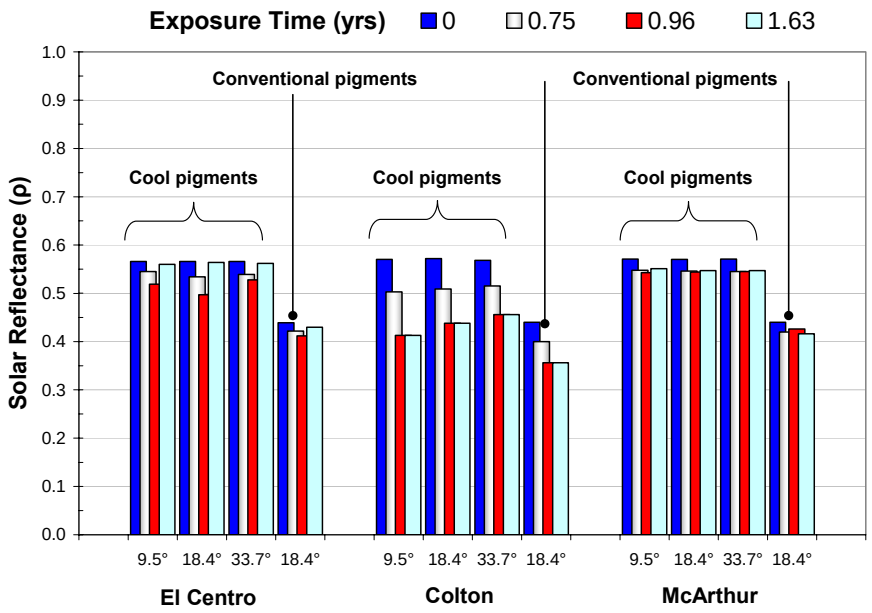

Fig. 7. Off-white (Rawhide) painted polyvinylidene fluoride metal with and without cool pigments. The slopes of 9.5º, 18.4º and 33.7º represent respective exposure settings of 2-in, 4-in and 8-in of rise per 12-in of run.

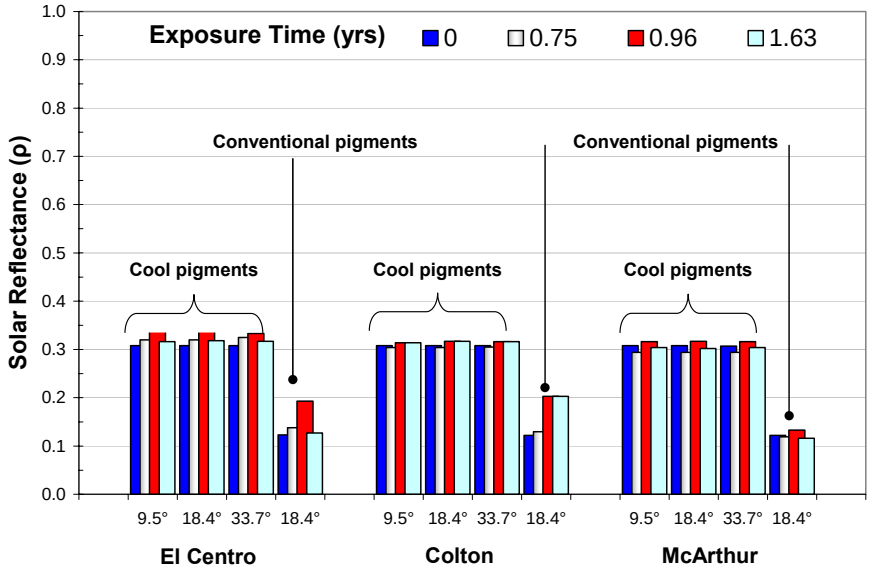

Fig. 8. Charcoal gray painted polyvinylidene fluoride metal with and without cool pigments. The slopes of 9.5º, 18.4º and 33.7º represent respective exposure settings of 2-in, 4-in and 8-in of rise per 12-in of run.

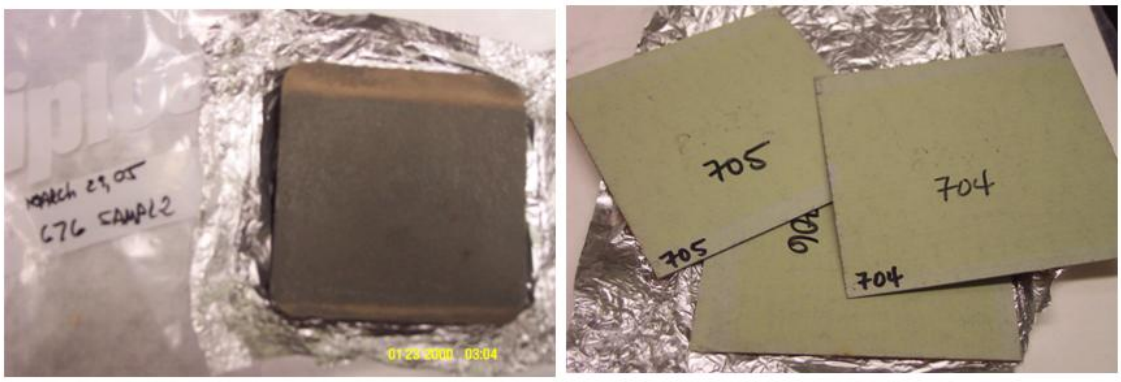

Fig. 9. Examples of concrete and painted metal roof samples analyzed for particulate matter and biomass.

Sonicating Bath

Fig. 10a. Sonicating bath of roof samples to extract particulate matter for chemical analysis

Filtration for Particulate Suspension

Fig. 10b. Filtration of extracted particulate matter for chemical analysis

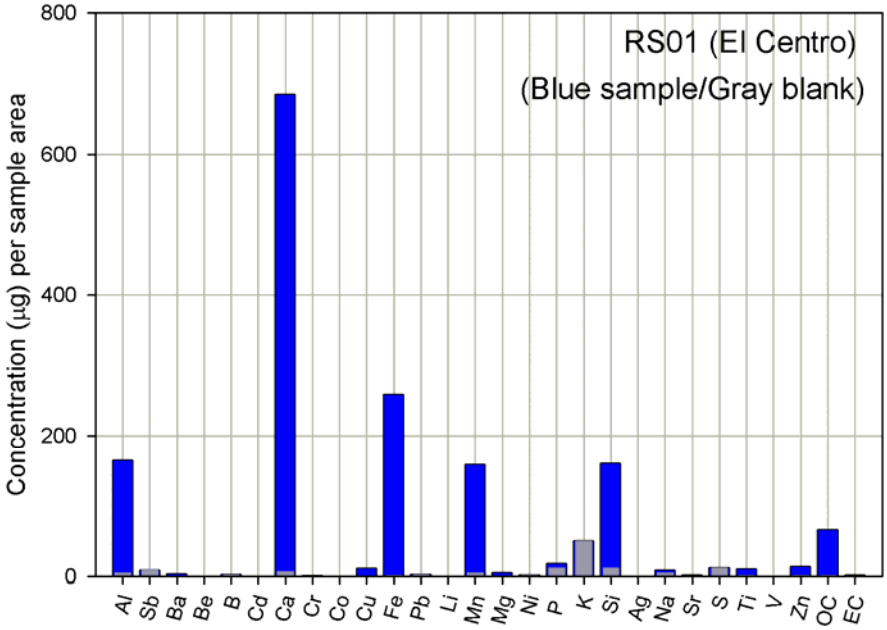

Fig. 11a. Chemical profile of particulate matter deposited on roof sample at El Centro site. Also shown in gray color is the chemical profile of the blank filter.Sample areas provided in Table 2.

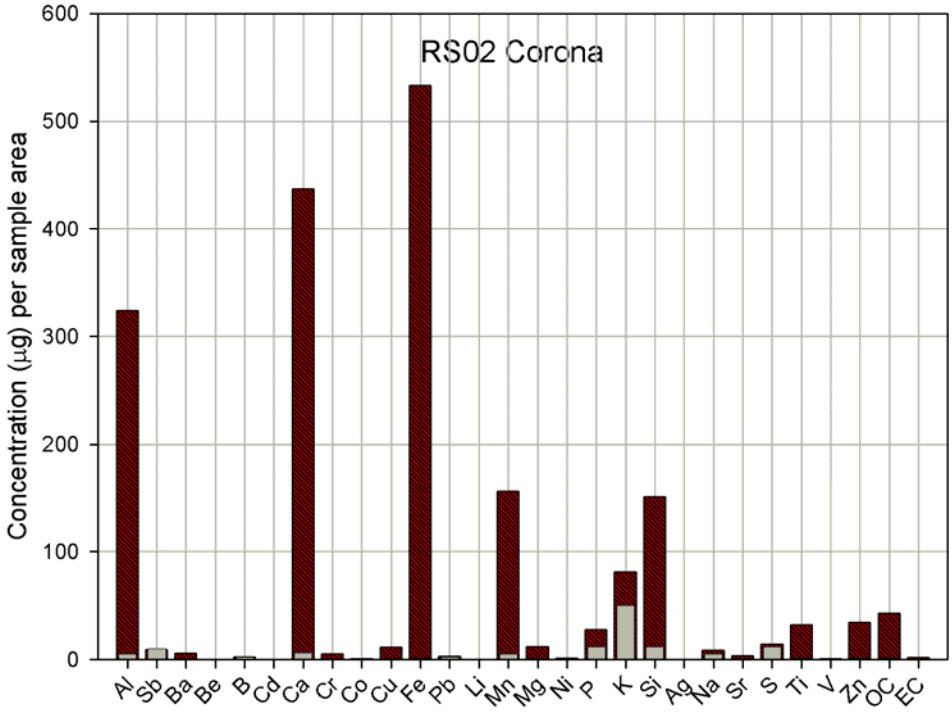

Fig. 11b. Chemical profile of particulate matter deposited on roof sample at Corona site. Also shown in gray color is the chemical profile of the blank filter.

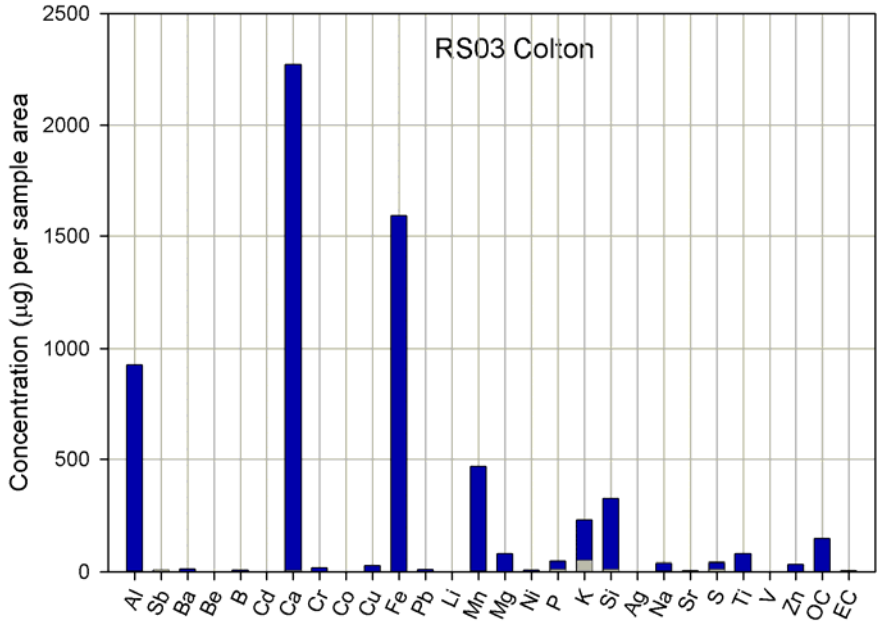

Fig. 11c. Chemical profile of particulate matter deposited on roof sample at Colton site. Also shown in gray color is the chemical profile of the blank filter.

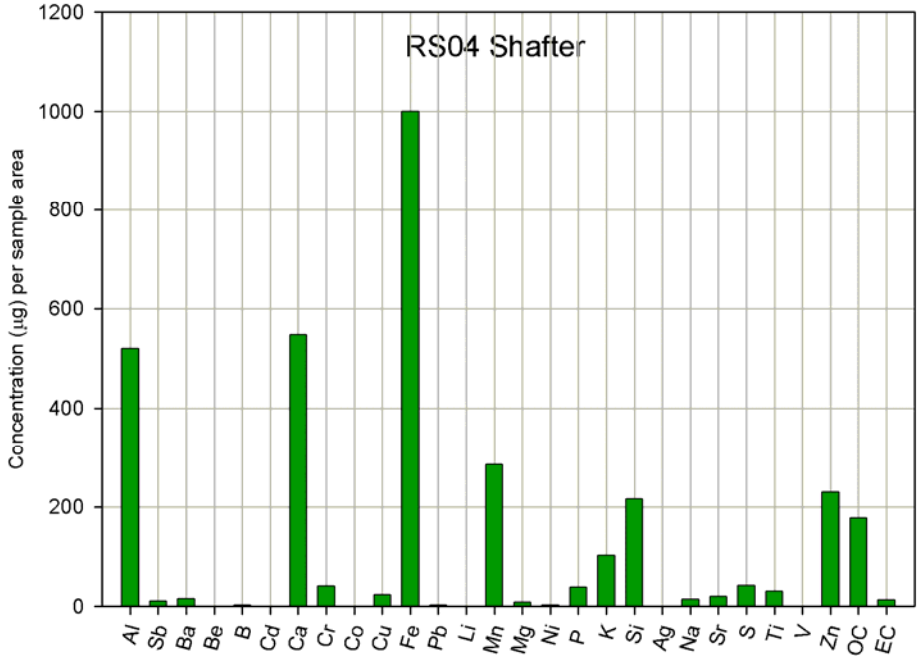

Fig. 11d. Chemical profile of particulate matter deposited on roof sample at Shafter site. Also shown in gray color is the chemical profile of the blank filter.

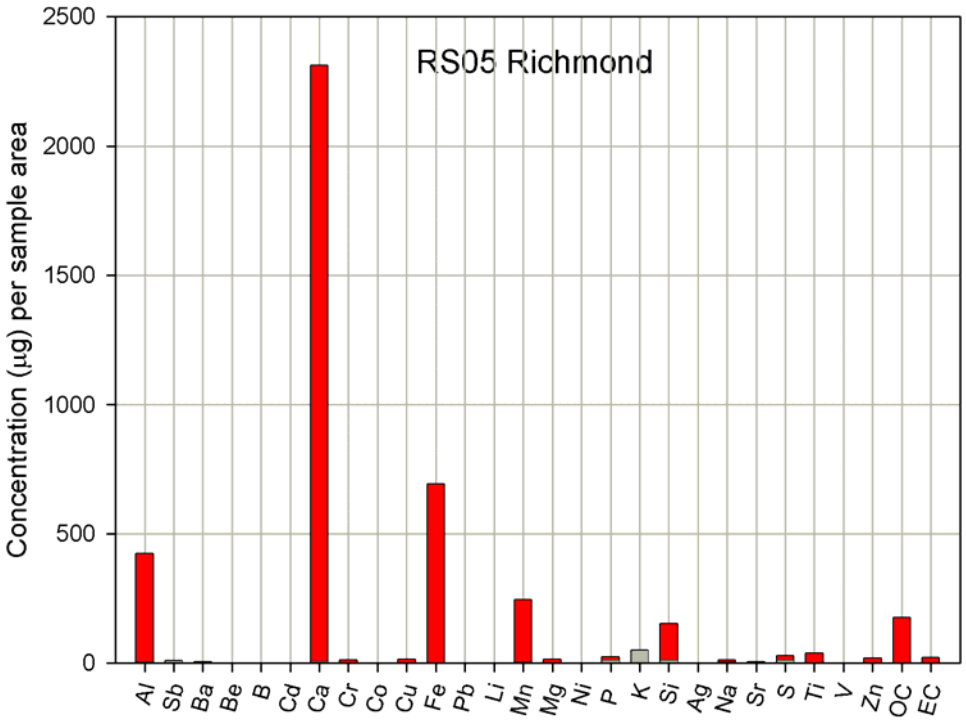

Fig. 11e. Chemical profile of particulate matter deposited on roof sample at Richmond site. Also shown in gray color is the chemical profile of the blank filter.

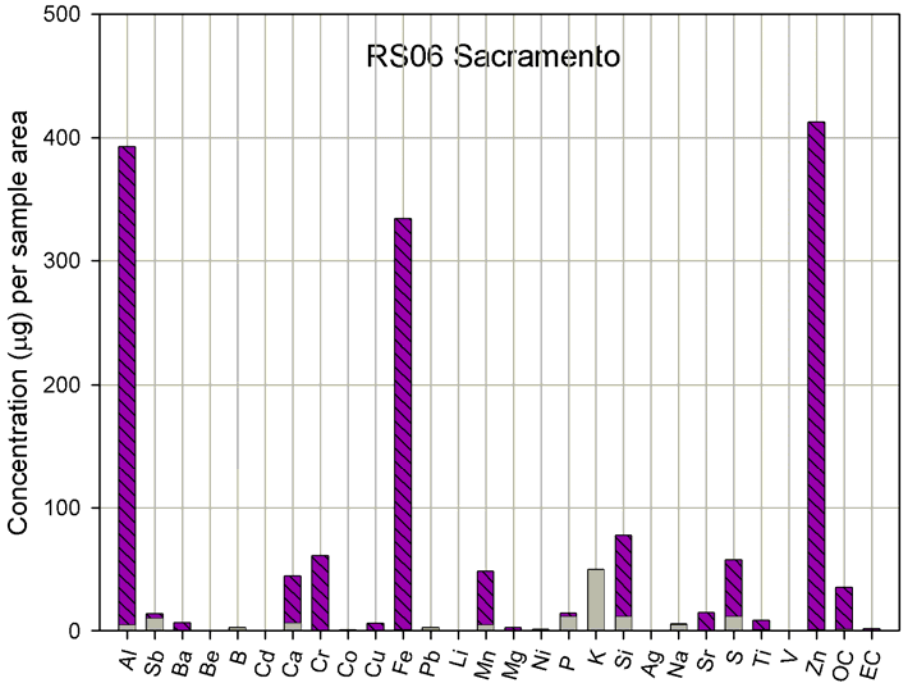

Fig. 11f. Chemical profile of particulate matter deposited on roof sample at Sacramento site. Also shown in gray color is the chemical profile of the blank filter.

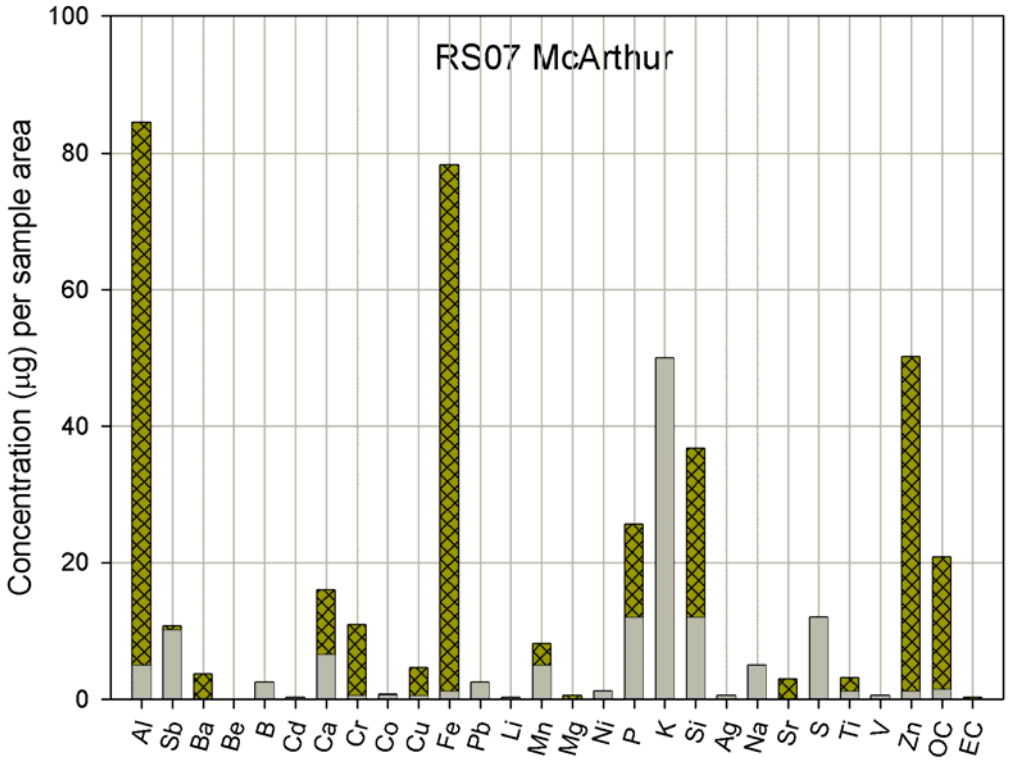

Fig. 11g. Chemical profile of particulate matter deposited on roof sample at McArthur site. Also shown in gray color is the chemical profile of the blank filter.

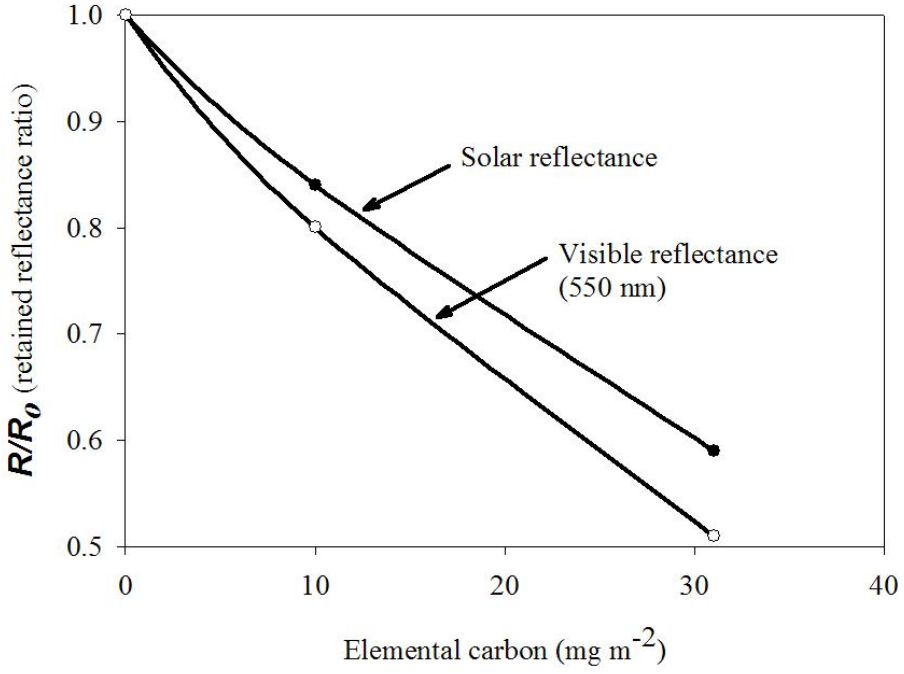

Fig. 12. Expected values for the soiled roof reflectance, divided by the unsoiled reflectance, as a function of elemental carbon (soot) concentration.

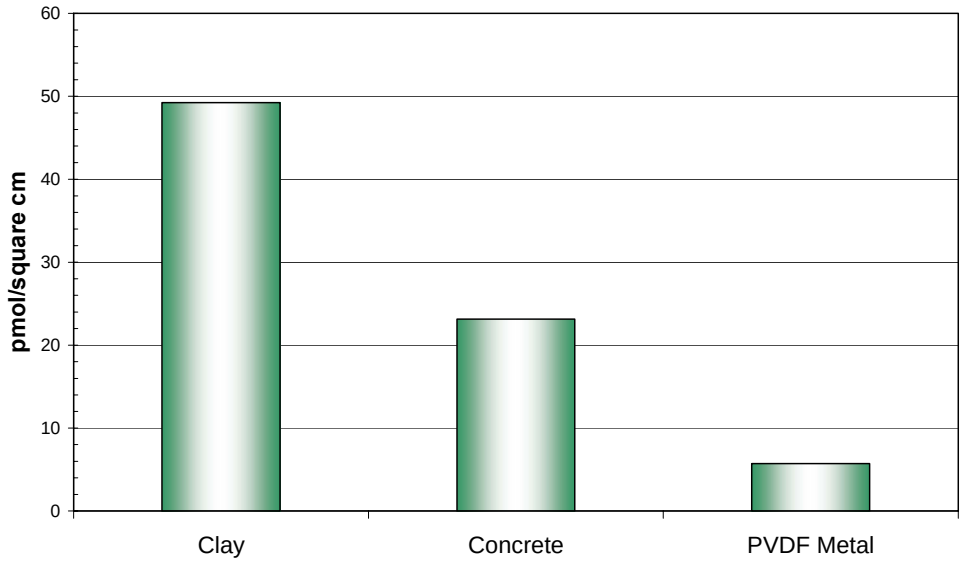

(b) PLFA average by material type

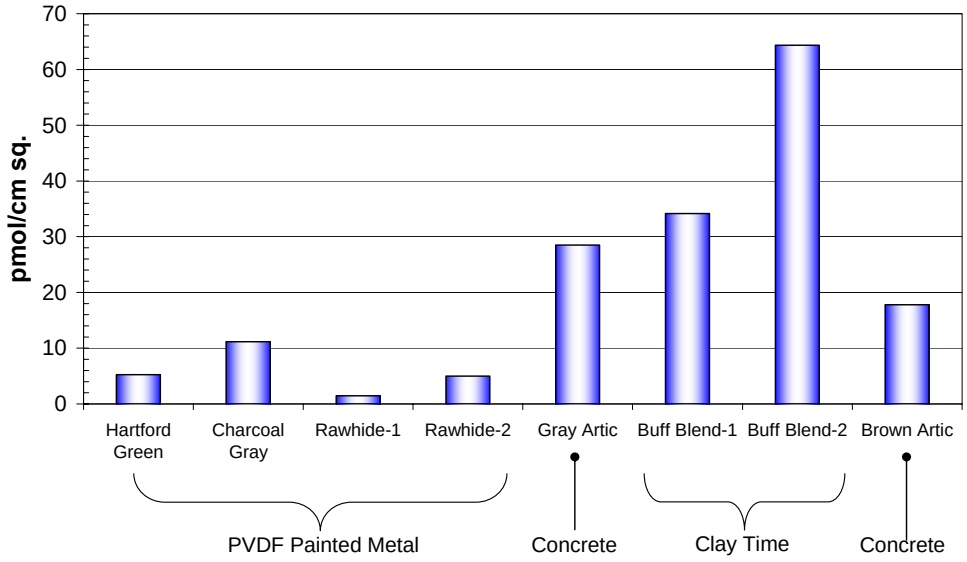

(a) PLFA estimates for each roof sample

Figure 13. Polar Lipid Fatty Acid (PLFA) estimates (a) for all roof samples and (b) averaged for the type of roof material; estimate units are pmol PLFA per square cm.

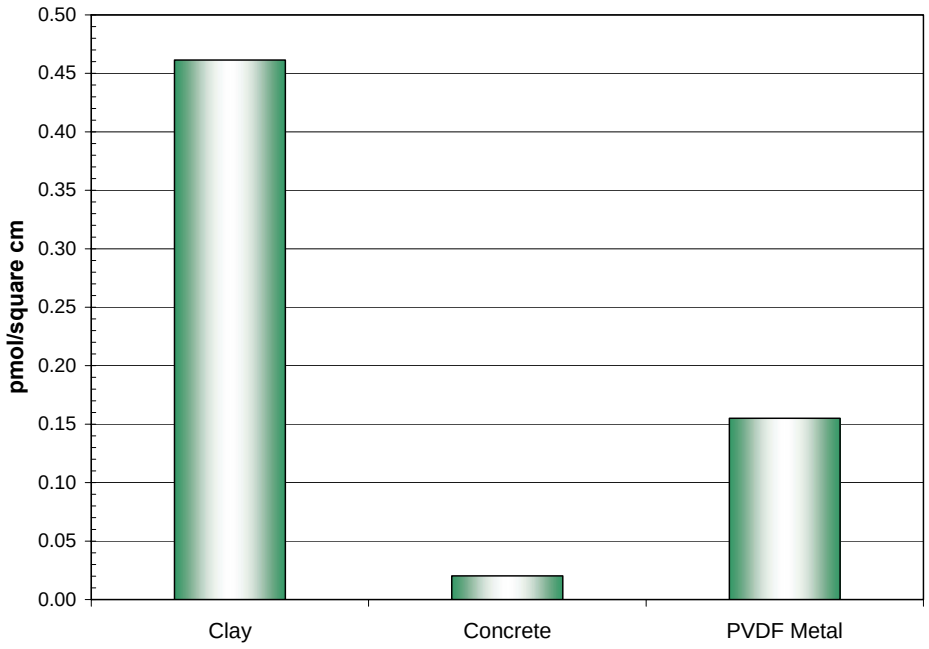

(b) Quinone averaged for type roof material.

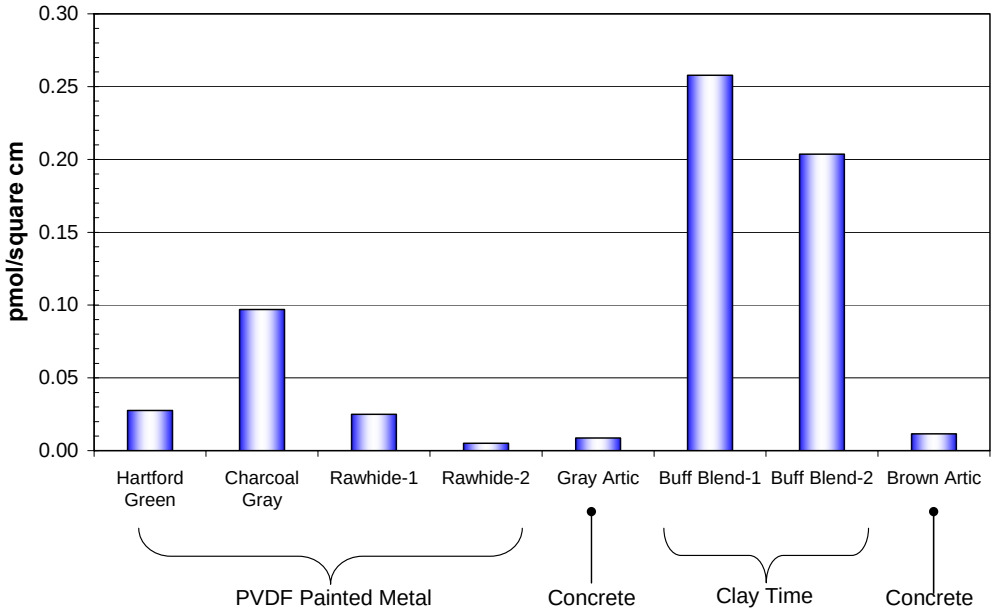

(a) Quinone for all roof samples.

Figure 14. Quinone estimates (a) for all roof samples and (b) averaged for the type of roof material; estimate units are pmol Quinone per square cm.

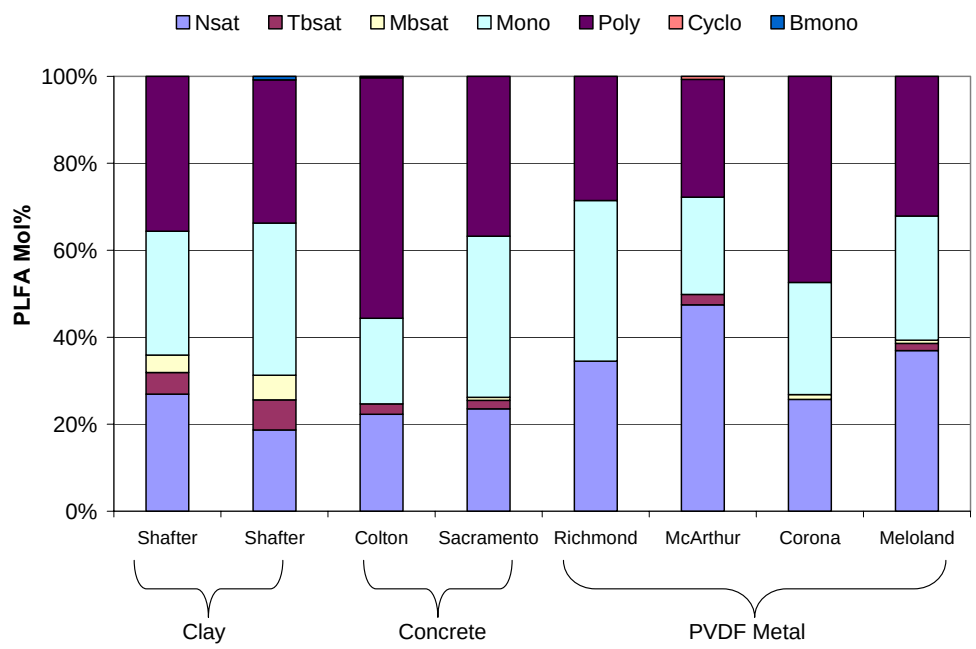

Figure 15. Community structure for the PLFA.

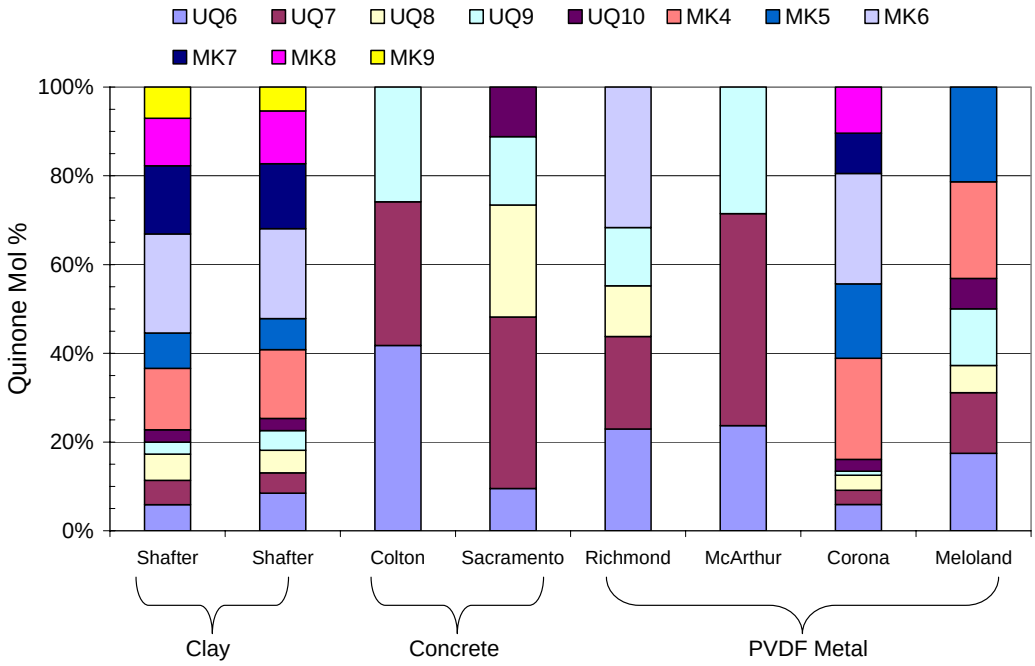

Figure 16. Quinone community composition.

Appendix A

El Centro Exposure Site (RS01)

Painted metal, clay and concrete tile roof products with and without cool color pigments were placed at ground level at the Davis University Agricultural Extension office located in El Centro, CA. Coupons of the roof products were installed in exposure rack assemblies, which are 5.5-ft high by 9-ft long, and divided into three sub-frames having respective slopes of 2-, 4- and 8-in of rise for 12-in of run (i.e., slopes of 9.5°, 18.4° and 33.7°). Each sub-frame can hold two "Sure-Grip" sub-assemblies, which are designed to have 6 rows of samples with 34-in of usable space in each row. Sample size is 3.5-in by 3.5-in. Orientation of the racks was set at 260° CCW and faced south, south-west into the sun. A CIMIS weather station (CIMIS # 87) is adjacent the exposure rack.

Figure A.1. Exposure rack ground mounted at University of Davis Agricultural Extension office, El Centro, CA.

El Centro, CA Solar Reflectance Field Data

Table A.1

				Exposure Time (yrs)				
	Identifier	**Code**	**Slope**	**0.000**	**0.742**	**0.962**	**1.625**	**2.488**
	BASF PVDF Painted Metal							
Regal White	872W2	900	2 in 12	0.740	0.664	0.551	0.724	0.609
	872W2	901	4 in 12	0.741	0.671	0.574	0.724	0.633
	872W2	902	8 in 12	0.740	0.697	0.653	0.722	0.647
	815W98	903	4 in 12	0.685	0.639	0.558	0.673	0.571
Rawhide	872T6	904	2 in 12	0.566	0.545	0.519	0.560	0.513
	872T6	905	4 in 12	0.566	0.534	0.497	0.564	0.521
	872T6	906	8 in 12	0.566	0.539	0.528	0.562	0.525
	836T223	907	4 in 12	0.439	0.422	0.412	0.430	0.410
Slate Blue	872B7	908	2 in 12	0.282	0.296	0.311	0.276	0.319
	872B7	909	4 in 12	0.282	0.297	0.321	0.276	0.308
	872B7	910	8 in 12	0.282	0.286	0.312	0.277	0.305
	815B49	911	4 in 12	0.169	0.192	0.243	0.173	0.240
Brick Red	872R10	912	2 in 12	0.374	0.379	0.384	0.382	0.400
	872R10	913	4 in 12	0.375	0.379	0.389	0.381	0.295
	872R10	914	8 in 12	0.373	0.380	0.389	0.383	0.397
	815R71	915	4 in 12	0.195	0.220	0.254	0.197	0.257
Charcoal Gray	872D6	916	2 in 12	0.308	0.320	0.342	0.316	0.358
	872D6	917	4 in 12	0.308	0.320	0.338	0.318	0.348
	872D6	918	8 in 12	0.308	0.325	0.333	0.317	0.347
	815D119	919	4 in 12	0.123	0.138	0.193	0.127	0.211
Hartford Green	872G16	920	2 in 12	0.270	0.288	0.318	0.276	
	872G16	921	4 in 12	0.272	0.290	0.319	0.276	
	872G16	922	8 in 12	0.274	0.295	0.290	0.280	
	815G37	923	4 in 12	0.088	0.134	0.176	0.094	
Slate Bronze	872T3	924	2 in 12	0.263	0.277	0.312	0.270	0.321
	872T3	925	4 in 12	0.262	0.283	0.304	0.270	0.315
	872T3	926	8 in 12	0.262	0.278	0.314	0.269	0.310
	815T119	927	4 in 12	0.118	0.155	0.250	0.123	0.211
	MCA Clay Tile							
White Buff	2F44	928	2 in 12	0.644	0.574	0.555	0.596	0.544
	2F44	929	4 in 12	0.638	0.567	0.554	0.581	0.539
	2F44	930	8 in 12	0.651	0.593	0.560	0.592	0.551
Apricot Buff	CF50	931	2 in 12	0.620	0.515	0.507	0.543	0.508
	CF50	932	4 in 12	0.598	0.546	0.545	0.574	0.543
	CF50	933	8 in 12	0.607	0.518	0.521	0.539	0.508
Adobe Gray	2F71	934	2 in 12	0.424	0.406	0.412	0.410	0.412
	2F71	935	4 in 12	0.421	0.409	0.414	0.419	0.414
	2F71	936	8 in 12	0.412	0.415	0.432	0.429	0.427
Regency Blue	2F52	937	2 in 12	0.411	0.395	0.398	0.395	0.395
	2F52	938	4 in 12	0.424	0.404	0.413	0.401	0.400
	2F52	939	8 in 12	0.422	0.402	0.409	0.392	0.401
Natural Red	F40	940	2 in 12	0.466	0.441	0.460	0.457	0.450
	F40	941	4 in 12	0.468	0.439	0.450		0.446
	F40	942	8 in 12	0.464	0.445	0.451	0.458	0.453
Weathered Green	B305	943	2 in 12	0.412	0.400	0.413	0.407	0.404
	B305	944	4 in 12	0.400	0.397	0.401	0.397	0.400
	B305	945	8 in 12	0.410	0.402	0.413	0.409	0.409
Ironwood	2F19	946	2 in 12	0.268	0.287	0.313	0.292	0.321
	2F19	947	4 in 12	0.271	0.300	0.315	0.296	0.321
	2F19	948	8 in 12	0.261	0.285	0.300	0.278	0.306
	US Clay Tile							
Buff Blend		979	2 in 12		0.568	0.543	0.568	0.549
Bermuda Blend		980	2 in 12		0.499	0.503	0.508	0.486
	Monierlife Concrete Roof Tile							
Terra Cotta Red	6978	949	2 in 12		0.184	0.268	0.181	0.229
	6978	950	4 in 12					
	6978	951	8 in 12					
Hearthside	3083	952	2 in 12		0.122	0.192	0.145	0.202
	3083	953	4 in 12		0.135	0.219	0.156	0.204
	3083	954	8 in 12		0.141	0.226	0.158	0.200
Riversidepebble	3080	955	2 in 12		0.164	0.225	0.166	0.214
	3080	956	4 in 12		0.131	0.202	0.140	0.189
	3080	957	8 in 12		0.136	0.219	0.154	0.200
Ebony	5047	958	2 in 12		0.133	0.257	0.130	0.188
	5047	959	4 in 12		0.136	0.242	0.156	0.187
	5047	960	8 in 12		0.134	0.219	0.129	0.177
Lincoln Green	4087	961	2 in 12		0.185	0.263	0.181	0.239
	4087	962	4 in 12		0.174	0.233	0.185	0.224
	4087	963	8 in 12		0.174	0.235	0.179	0.217

El Centro, CA Solar Reflectance Field Data

Table A.1

				Exposure Time (yrs)				
	Identifier	**Code**	**Slope**	**0.000**	**0.742**	**0.962**	**1.625**	**2.488**
	Shepherd Artic Match							
Blue Artic		964	2 in 12		0.226	0.285	0.237	0.285
		965	4 in 12		0.234	0.295	0.243	0.277
		966	8 in 12		0.225	0.299	0.235	0.269
Red Artic		967	2 in 12		0.267	0.317	0.279	0.316
		968	4 in 12		0.266	0.318	0.283	0.316
		969	8 in 12		0.309	0.339	0.306	0.338
Brown Artic		970	2 in 12		0.261	0.315	0.283	0.320
		971	4 in 12		0.260	0.315	0.283	0.313
		972	8 in 12		0.251	0.315	0.283	
Black Artic		973	2 in 12		0.260	0.311	0.262	0.298
		974	4 in 12		0.229	0.287	0.229	0.268
		975	8 in 12		0.247	0.299	0.242	0.272
Gray Artic		976	2 in 12		0.265	0.328	0.275	
		977	4 in 12		0.274	0.316	0.286	0.324
		978	8 in 12		0.278	0.323	0.294	
	American Roof Coatings							
NIR3704	Ultra Marine	981	8 in 12		0.389	0.382	0.397	0.396
IR3808	Chocolate	982	8 in 12		0.411	0.408	0.409	0.413
IR3503	Camo Green	983	8 in 12		0.467	0.456	0.460	0.454
IR3108	Light Gray	984	8 in 12		0.432	0.417	0.426	0.421
IR3308	Terracotta	985	8 in 12		0.473	0.455	0.476	0.421
NIR3900	Onyx	986	8 in 12		0.406	0.453	0.467	0.463

Appendix A

Corona Exposure Site (RS02)

Painted metal, clay and concrete tile roof products with and without cool color pigments were placed at ground level adjacent the clay tile manufacturing facility of Maruhachi Ceramics of America, Inc. located in Corona, CA. Coupons of the roof products were installed in exposure rack assemblies, which are 5.5-ft high by 9-ft long, and divided into three sub-frames having respective slopes of 2-, 4- and 8-in of rise for 12-in of run (i.e., slopes of 9.5°, 18.4° and 33.7°). Each sub-frame can hold two "Sure-Grip" sub-assemblies, which are designed to have 6 rows of samples with 34-in of usable space in each row. Sample size is 3.5-in by 3.5-in. Orientation of the racks is 310° CCW from the east and faces south south-east.

Figure A.2. Exposure rack ground mounted at Corona, CA.

Corona, CA Solar Reflectance Field Data

Table A.2

				Exposure Time (yrs)				
	Identifier	**Code**	**Slope**	**0.000**	**0.745**	**0.962**	**1.630**	**2.493**
	BASF PVDF Painted Metal							
Regal White	872W2	600	2 in 12	0.740	0.691	0.542	0.675	0.604
	872W2	601	4 in 12	0.739	0.692	0.605	0.671	0.604
	872W2	602	8 in 12	0.740	0.693	0.651	0.688	0.634
	815W98	603	4 in 12	0.687	0.649	0.566	0.620	0.574
Rawhide	872T6	604	2 in 12	0.573	0.532	0.468	0.518	0.489
	872T6	605	4 in 12	0.573	0.534	0.496	0.522	0.503
	872T6	606	8 in 12	0.569	0.535	0.498	0.524	0.508
	836T223	607	4 in 12	0.440	0.417	0.386	0.395	0.384
Slate Blue	872B7	608	2 in 12	0.282	0.278	0.282	0.259	0.278
	872B7	609	4 in 12	0.281	0.278	0.285	0.259	0.278
	872B7	610	8 in 12	0.282	0.279	0.279	0.262	0.277
	815B49	611	4 in 12	0.172	0.175	0.202	0.165	0.197
Brick Red	872R10	612	2 in 12	0.372	0.363	0.358	0.356	0.365
	872R10	613	4 in 12	0.374	0.364	0.360	0.358	0.368
	872R10	614	8 in 12	0.375	0.363	0.363	0.359	0.370
	815R71	615	4 in 12	0.195	0.198	0.222	0.190	0.223
Charcoal Gray	872D6	616	2 in 12	0.309	0.305	0.314	0.297	
	872D6	617	4 in 12	0.309	0.305	0.304	0.300	0.319
	872D6	618	8 in 12	0.308	0.304	0.305	0.300	0.318
	815D119	619	4 in 12	0.122	0.129	0.164	0.120	0.162
Hartford Green	872G16	620	2 in 12	0.271	0.271	0.289	0.263	0.286
	872G16	621	4 in 12	0.272	0.271	0.280	0.266	0.288
	872G16	622	8 in 12	0.272	0.268	0.274	0.263	
	815G37	623	4 in 12	0.089	0.097	0.142	0.095	0.137
Slate Bronze	872T3	624	2 in 12	0.262	0.261	0.280	0.253	0.278
	872T3	625	4 in 12	0.263	0.263	0.276	0.256	0.280
	872T3	626	8 in 12	0.262	0.262	0.266	0.257	0.278
	815T119	627	4 in 12	0.118	0.124	0.167	0.119	0.161
	MCA Clay Tile							
White Buff	2F44	628	2 in 12	0.640	0.560	0.482	0.526	0.458
	2F44	629	4 in 12	0.651	0.568	0.503	0.536	0.484
	2F44	630	8 in 12	0.632	0.584	0.538	0.550	0.514
Apricot Buff	CF50	631	2 in 12	0.601	0.547	0.482	0.514	0.433
	CF50	632	4 in 12	0.595	0.539	0.477	0.510	0.469
	CF50	633	8 in 12	0.619	0.549	0.558	0.527	0.497
Adobe Gray	2F71	634	2 in 12	0.426	0.414	0.385	0.393	0.366
	2F71	635	4 in 12	0.418	0.420	0.387	0.395	0.383
	2F71	636	8 in 12	0.420	0.400	0.392	0.389	0.380
Regency Blue	2F52	637	2 in 12	0.420	0.395	0.368	0.365	0.338
	2F52	638	4 in 12	0.412	0.388	0.366	0.355	0.350
	2F52	639	8 in 12	0.406	0.396	0.377	0.371	0.361
Natural Red	F40	640	2 in 12	0.449	0.415	0.393	0.395	
	F40	641	4 in 12	0.462	0.430	0.415	0.408	0.394
	F40	642	8 in 12	0.459	0.423	0.430	0.415	0.407
Weathered Green	B305	643	2 in 12	0.411	0.386	0.346	0.357	
	B305	644	4 in 12	0.419	0.378	0.348	0.357	0.340
	B305	645	8 in 12	0.409	0.390	0.385	0.378	0.372
Ironwood	2F19	646	2 in 12	0.267	0.253	0.264	0.240	
	2F19	647	4 in 12	0.273	0.252	0.267	0.245	0.272
	2F19	648	8 in 12	0.270	0.253	0.255	0.257	0.275
	US Clay Tile							
Buff Blend		679	2 in 12		0.536	0.272	0.492	0.436
Bermuda Blend		680	2 in 12		0.456	0.278	0.411	0.396
	Monierlife Concrete Roof Tile							
Terra Cotta Red	6978	649	2 in 12		0.206	0.233	0.197	0.228
	6978	650	4 in 12		0.207	0.209	0.195	0.235
	6978	651	8 in 12		0.178	0.182	0.165	0.212
Hearthside	3083	652	2 in 12		0.143	0.186	0.158	0.196
	3083	653	4 in 12		0.131	0.134	0.166	0.217
	3083	654	8 in 12		0.125	0.138	0.164	0.207
Riversidepebble	3080	655	2 in 12		0.146	0.171	0.164	0.215
	3080	656	4 in 12		0.151	0.142	0.199	0.222
	3080	657	8 in 12		0.151	0.141	0.156	0.200
Ebony	5047	658	2 in 12		0.140	0.186	0.141	0.192
	5047	659	4 in 12		0.131	0.130	0.128	0.176
	5047	660	8 in 12		0.137	0.135	0.125	0.172
Lincoln Green	4087	661	2 in 12		0.169	0.211	0.178	0.227
	4087	662	4 in 12		0.161	0.140	0.174	0.217
	4087	663	8 in 12		0.165	0.164	0.171	0.203

Corona, CA Solar Reflectance Field Data

Table A.2

				Exposure Time (yrs)				
	Identifier	**Code**	**Slope**	**0.000**	**0.745**	**0.962**	**1.630**	**2.493**
	Shepherd Artic Match							
Blue Artic		664	2 in 12		0.255	0.270	0.251	0.257
		665	4 in 12		0.258	0.273	0.249	0.265
		666	8 in 12		0.250	0.262	0.238	0.250
Red Artic		667	2 in 12		0.273	0.283	0.261	0.269
		668	4 in 12		0.270		0.266	0.281
		669	8 in 12		0.276	0.287	0.262	0.279
Brown Artic		670	2 in 12		0.255	0.282	0.253	0.262
		671	4 in 12		0.244	0.268	0.247	0.263
		672	8 in 12		0.258	0.277	0.266	0.278
Black Artic		673	2 in 12		0.230	0.258	0.212	0.249
		674	4 in 12		0.228			0.240
		675	8 in 12		0.234	0.236	0.217	0.238
Gray Artic		676	2 in 12		0.252	0.272	0.233	0.254
		677	4 in 12		0.243		0.249	0.264
		678	8 in 12		0.251	0.278	0.250	0.271
	American Roof Coatings							
NIR3704	Ultra Marine	681	4 in 12		0.383	0.379	0.362	0.367
IR3808	Chocolate	682	4 in 12		0.410	0.395	0.387	0.387
IR3503	Camo Green	683	4 in 12		0.467	0.448	0.435	0.429
IR3108	Light Gray	684	4 in 12		0.438	0.415	0.400	0.395
IR3308	Terracotta	685	4 in 12		0.474	0.463	0.443	0.439
NIR3900	Onyx	686	4 in 12		0.432	0.463	0.434	0.417

Appendix A

Colton Exposure Site (RS03)

Painted metal, clay and concrete tile roof products with and without cool color pigments were placed on top of the low-slope roof at BASF's Research plant in Colton, CA. Coupons of the roof products were installed in exposure rack assemblies, which are 5.5-ft high by 9-ft long, and divided into three sub-frames having respective slopes of 2-, 4- and 8-in of rise for 12-in of run (i.e., slopes of 9.5°, 18.4° and 33.7°). Each sub-frame can hold two "Sure-Grip" sub-assemblies, which are designed to have 6 rows of samples with 34-in of usable space in each row. Sample size is 3.5-in by 3.5-in. Orientation of the racks was set at 270° CCW from the east, so the roof coupons faced directly south to receive full solar exposure.

Figure A.3. Exposure rack mounted on the low-slope roof of BASF's Research facility in Colton, CA.

Colton, CA Solar Reflectance Field Data

Table A.3

				Exposure Time (yrs)				
	Identifier	**Code**	**Slope**	**0.000**	**0.748**	**0.962**	**1.630**	**2.493**
	BASF PVDF Painted Metal							
Regal White	872W2	500	2.628 in 12	0.742	0.646	0.491	0.673	0.639
	872W2	501	4.628 in 12	0.742	0.649	0.537	0.677	0.642
	872W2	502	8.628 in 12	0.743	0.663	0.537	0.681	0.658
	815W98	503	4.628 in 12	0.689	0.602	0.513	0.625	0.602
Rawhide	872T6	504	2.628 in 12	0.570	0.503	0.413	0.521	0.504
	872T6	505	4.628 in 12	0.572	0.509	0.438	0.520	0.515
	872T6	506	8.628 in 12	0.568	0.515	0.456	0.528	0.524
	836T223	507	4.628 in 12	0.440	0.400	0.356	0.400	0.399
Slate Blue	872B7	508	2.628 in 12	0.283	0.276	0.289	0.257	0.272
	872B7	509	4.628 in 12	0.282	0.278	0.290	0.258	0.271
	872B7	510	8.628 in 12	0.283	0.278	0.290	0.257	0.271
	815B49	511	4.628 in 12	0.173	0.185	0.227	0.162	0.181
Brick Red	872R10	512	2.628 in 12	0.375	0.354	0.343	0.353	0.363
	872R10	513	4.628 in 12	0.374	0.355	0.349	0.353	0.365
	872R10	514	8.628 in 12	0.374	0.358	0.349	0.355	0.362
	815R71	515	4.628 in 12	0.195	0.205	0.250	0.186	0.206
Charcoal Gray	872D6	516	2.628 in 12	0.308	0.304	0.314	0.297	0.312
	872D6	517	4.628 in 12	0.308	0.304	0.317	0.297	
	872D6	518	8.628 in 12	0.308	0.305	0.316	0.297	
	815D119	519	4.628 in 12	0.122	0.130	0.203	0.117	
Hartford Green	872G16	520	2.628 in 12	0.272	0.271	0.296	0.254	0.276
	872G16	521	4.628 in 12	0.272	0.273	0.294	0.260	0.277
	872G16	522	8.628 in 12	0.273	0.271	0.294	0.260	0.275
	815G37	523	4.628 in 12	0.089	0.116	0.189	0.088	0.113
Slate Bronze	872T3	524	2.628 in 12	0.262	0.263	0.293	0.251	0.268
	872T3	525	4.628 in 12	0.263	0.264	0.290	0.252	0.270
	872T3	526	8.628 in 12	0.262	0.264	0.287	0.249	0.268
	815T119	527	4.628 in 12	0.118	0.140	0.206	0.115	0.139
	MCA Clay Tile							
White Buff	2F44	528	2.628 in 12	0.647	0.543	0.456	0.559	0.509
	2F44	529	4.628 in 12	0.653	0.554	0.479	0.565	0.523
	2F44	530	8.628 in 12	0.643	0.555	0.482	0.568	0.541
Apricot Buff	CF50	531	2.628 in 12	0.609	0.555	0.472	0.560	0.491
	CF50	532	4.628 in 12	0.611	0.563	0.496	0.576	0.505
	CF50	533	8.628 in 12	0.604	0.519	0.459	0.536	0.506
Adobe Gray	2F71	534	2.628 in 12	0.434	0.361	0.344	0.364	0.352
	2F71	535	4.628 in 12	0.460	0.378	0.359	0.380	0.369
	2F71	536	8.628 in 12	0.449	0.384	0.363	0.386	0.383
Regency Blue	2F52	537	2.628 in 12	0.435	0.379	0.351	0.367	0.351
	2F52	538	4.628 in 12	0.424	0.380	0.355	0.368	0.357
	2F52	539	8.628 in 12	0.430	0.381	0.359	0.369	0.368
Natural Red	F40	540	2.628 in 12	0.461	0.421	0.397	0.423	0.413
	F40	541	4.628 in 12	0.463	0.416	0.389	0.412	0.405
	F40	542	8.628 in 12	0.465	0.418	0.395	0.419	0.417
Weathered Green	B305	543	2.628 in 12	0.405	0.377	0.352	0.377	0.353
	B305	544	4.628 in 12	0.406	0.363	0.341	0.360	0.337
	B305	545	8.628 in 12	0.411	0.358	0.332	0.353	0.336
Ironwood	2F19	546	2.628 in 12	0.270	0.254	0.273	0.240	0.252
	2F19	547	4.628 in 12	0.268	0.253	0.272	0.240	0.252
	2F19	548	8.628 in 12	0.267	0.258	0.271	0.244	0.256
	US Clay Tile							
Buff Blend		579	2.628 in 12		0.514	0.465	0.489	0.471
Bermuda Blend		580	2.628 in 12		0.481	0.455	0.472	0.468
	Monierlife Concrete Roof Tile							
Terra Cotta Red	6978	549	2.628 in 12		0.200	0.230	0.192	0.219
	6978	550	4.628 in 12		0.195	0.222	0.181	0.210
	6978	551	8.628 in 12		0.202	0.226	0.176	0.206
Hearthside	3083	552	2.628 in 12		0.149	0.202	0.178	0.207
	3083	553	4.628 in 12		0.138	0.200	0.158	0.193
	3083	554	8.628 in 12		0.135	0.207	0.161	0.190
Riversidepebble	3080	555	2.628 in 12		0.141	0.195	0.171	0.197
	3080	556	4.628 in 12		0.141	0.201	0.172	0.199
	3080	557	8.628 in 12		0.154	0.196	0.148	0.186
Ebony	5047	558	2.628 in 12		0.139	0.187	0.134	0.167
	5047	559	4.628 in 12		0.130	0.189	0.131	0.160
	5047	560	8.628 in 12		0.143	0.193	0.125	0.155
Lincoln Green	4087	561	2.628 in 12		0.180	0.226	0.172	0.197
	4087	562	4.628 in 12		0.153	0.204	0.152	
	4087	563	8.628 in 12		0.175	0.211	0.169	0.203

Colton, CA Solar Reflectance Field Data

Table A.3

				Exposure Time (yrs)				
	Identifier	Code	Slope	0.000	0.748	0.962	1.630	2.493
	Shepherd Artic Match							
Blue Artic		564	2.628 in 12		0.234	0.260	0.222	0.232
		565	4.628 in 12		0.242	0.270	0.229	0.238
		566	8.628 in 12		0.250	0.276	0.242	0.263
Red Artic		567	2.628 in 12		0.265	0.279	0.256	0.254
		568	4.628 in 12		0.276	0.287	0.263	0.264
		569	8.628 in 12		0.311	0.302	0.273	0.289
Brown Artic		570	2.628 in 12		0.250	0.281	0.260	0.263
		571	4.628 in 12		0.265	0.290	0.258	0.266
		572	8.628 in 12		0.266	0.283	0.266	0.276
Black Artic		573	2.628 in 12		0.233	0.265	0.208	0.229
		574	4.628 in 12		0.245	0.264	0.215	0.230
		575	8.628 in 12		0.223	0.255	0.197	0.220
Gray Artic		576	2.628 in 12		0.246	0.277	0.241	
		577	4.628 in 12		0.252	0.277	0.256	
		578	8.628 in 12		0.276	0.286	0.256	0.267
	American Roof Coatings							
NIR3704	Ultra Marine	581	4 in 12		0.369	0.343	0.355	0.358
IR3808	Chocolate	582	4 in 12		0.411	0.365	0.377	0.385
IR3503	Camo Green	583	4 in 12		0.466	0.392	0.426	0.428
IR3108	Light Gray	584	4 in 12		0.433	0.367	0.391	0.392
IR3308	Terracotta	585	4 in 12		0.474	0.403	0.433	0.433
NIR3900	Onyx	586	4 in 12		0.430	0.424	0.426	0.413

Appendix A

Shafter Exposure Site (RS04)

Painted metal, clay and concrete tile roof products with and without cool color pigments were placed at ground level on the premises of Elk Corp.'s manufacturing facility in Shafter, CA. Coupons of the roof products were installed in exposure rack assemblies, which are 5.5-ft high by 9-ft long, and divided into three sub-frames having respective slopes of 2-, 4- and 8-in of rise for 12-in of run (i.e., slopes of 9.5°, 18.4° and 33.7°). Each sub-frame can hold two "Sure-Grip" sub-assemblies, which are designed to have 6 rows of samples with 34-in of usable space in each row. Sample size is 3.5-in by 3.5-in. Orientation of the racks was set at 270° CCW from the east, so the roof coupons faced directly south to receive full solar exposure.

Figure A.4. Exposure rack mounted on the ground at Elk Corp.'s Manufacturing facility in Shafter, CA.

Shafter, CA Solar Reflectance Field Data

Table A.4

				Exposure Time (yrs)				
	Identifier	**Code**	**Slope**	**0.000**	**0.751**	**0.959**	**1.633**	**2.496**
	BASF PVDF Painted Metal							
Regal White	872W2	700	2 in 12	0.739	0.613	0.529	0.687	0.596
	872W2	701	4 in 12	0.742	0.559	0.589	0.685	0.623
	872W2	702	8 in 12	0.737	0.591	0.558	0.689	0.617
	815W98	703	4 in 12	0.688	0.551	0.545	0.638	0.574
Rawhide	872T6	704	2 in 12	0.570	0.490	0.443	0.524	
	872T6	705	4 in 12	0.569	0.456	0.457	0.523	
	872T6	706	8 in 12	0.574	0.469	0.437	0.525	
	836T223	707	4 in 12	0.441	0.378	0.369	0.405	
Slate Blue	872B7	708	2 in 12	0.282	0.278	0.277	0.256	0.256
	872B7	709	4 in 12	0.283	0.279	0.278	0.258	0.261
	872B7	710	8 in 12	0.282	0.278	0.280	0.258	0.262
	815B49	711	4 in 12	0.172	0.199	0.204	0.158	0.176
Brick Red	872R10	712	2 in 12	0.375	0.350	0.340	0.353	0.339
	872R10	713	4 in 12	0.375	0.344	0.347	0.354	0.348
	872R10	714	8 in 12	0.375	0.340	0.338	0.353	0.350
	815R71	715	4 in 12	0.195	0.220	0.218	0.184	0.200
Charcoal Gray	872D6	716	2 in 12	0.308	0.303	0.307	0.295	0.296
	872D6	717	4 in 12	0.308	0.304	0.303	0.295	0.299
	872D6	718	8 in 12	0.308	0.304	0.305	0.297	0.301
	815D119	719	4 in 12	0.122	0.175	0.163	0.116	0.141
Hartford Green	872G16	720	2 in 12	0.270	0.276	0.279	0.258	0.262
	872G16	721	4 in 12	0.272	0.278	0.279	0.260	0.267
	872G16	722	8 in 12	0.271	0.273	0.279	0.260	0.266
	815G37	723	4 in 12	0.088	0.154	0.151	0.086	0.114
Slate Bronze	872T3	724	2 in 12	0.262	0.269	0.273	0.250	0.258
	872T3	725	4 in 12	0.263	0.269	0.273	0.250	0.258
	872T3	726	8 in 12	0.262	0.270	0.277	0.250	0.257
	815T119	727	4 in 12	0.188	0.161	0.180	0.113	0.137
	MCA Clay Tile							
White Buff	2F44	728	2 in 12	0.626	0.503	0.482	0.541	0.476
	2F44	729	4 in 12	0.645	0.487	0.488	0.536	0.473
	2F44	730	8 in 12	0.637	0.505	0.491	0.556	0.488
Apricot Buff	CF50	731	2 in 12	0.644	0.489	0.451	0.513	0.440
	CF50	732	4 in 12	0.652	0.448	0.438	0.505	0.468
	CF50	733	8 in 12	0.606	0.458	0.454	0.522	0.470
Adobe Gray	2F71	734	2 in 12	0.406	0.367	0.358	0.369	0.347
	2F71	735	4 in 12	0.424	0.363	0.359	0.373	0.354
	2F71	736	8 in 12	0.428	0.352	0.358	0.371	0.344
Regency Blue	2F52	737	2 in 12	0.414	0.367	0.366	0.343	0.317
	2F52	738	4 in 12	0.413	0.360	0.367	0.359	0.328
	2F52	739	8 in 12	0.407	0.360	0.382	0.364	0.339
Natural Red	F40	740	2 in 12	0.470	0.415	0.413	0.407	0.368
	F40	741	4 in 12	0.457	0.410	0.429	0.407	0.380
	F40	742	8 in 12	0.460	0.409	0.401	0.414	0.382
Weathered Green	B305	743	2 in 12	0.425	0.362	0.341	0.369	0.345
	B305	744	4 in 12	0.406	0.333	0.328	0.352	0.329
	B305	745	8 in 12	0.401	0.334	0.334	0.364	0.339
Ironwood	2F19	746	2 in 12	0.266	0.260	0.275	0.231	0.240
	2F19	747	4 in 12	0.267	0.267	0.273	0.237	0.247
	2F19	748	8 in 12	0.270	0.262	0.274	0.235	0.241
	US Clay Tile							
Buff Blend		779	2 in 12		0.565	0.486	0.521	
Bermuda Blend		780	2 in 12		0.489	0.436	0.447	
	Monierlife Concrete Roof Tile							
Terra Cotta Red	6978	749	2 in 12		0.202	0.238	0.172	0.189
	6978	750	4 in 12		0.181	0.226	0.154	0.173
	6978	751	8 in 12		0.216	0.235	0.168	0.183
Hearthside	3083	752	2 in 12		0.121	0.196	0.136	0.162
	3083	753	4 in 12		0.125	0.194	0.142	0.184
	3083	754	8 in 12		0.131	0.199	0.144	0.164
Riversidepebble	3080	755	2 in 12		0.142	0.185	0.134	0.167
	3080	756	4 in 12		0.165	0.197	0.164	0.178
	3080	757	8 in 12		0.148	0.187	0.148	0.178
Ebony	5047	758	2 in 12		0.137	0.199	0.112	0.142
	5047	759	4 in 12		0.141	0.197	0.109	0.137
	5047	760	8 in 12		0.141	0.191	0.111	0.137
Lincoln Green	4087	761	2 in 12		0.155	0.210	0.151	0.170
	4087	762	4 in 12		0.177	0.217	0.157	0.189
	4087	763	8 in 12		0.185	0.218	0.161	0.186

Shafter, CA Solar Reflectance Field Data

Table A.4

				Exposure Time (yrs)				
	Identifier	Code	Slope	0.000	0.751	0.959	1.633	2.496
	Shepherd Artic Match							
Blue Artic		764	2 in 12		0.246	0.262	0.238	0.230
		765	4 in 12		0.237	0.249	0.220	0.229
		766	8 in 12		0.226	0.251	0.206	0.217
Red Artic		767	2 in 12		0.312	0.294	0.377	0.279
		768	4 in 12		0.331	0.297	0.313	0.316
		769	8 in 12		0.321	0.297	0.302	0.299
Brown Artic		770	2 in 12		0.251	0.264	0.250	0.242
		771	4 in 12		0.259	0.266	0.253	0.253
		772	8 in 12		0.260	0.263	0.248	0.248
Black Artic		773	2 in 12		0.240	0.256	0.203	0.213
		774	4 in 12		0.231	0.252	0.210	0.221
		775	8 in 12		0.213	0.239	0.196	0.206
Gray Artic		776	2 in 12		0.257	0.260	0.247	0.241
		777	4 in 12		0.272	0.265	0.246	0.256
		778	8 in 12		0.248	0.259	0.238	0.239
	American Roof Coatings							
NIR3704	Ultra Marine	781	4 in 12		0.385	0.338	0.364	0.350
IR3808	Chocolate	782	4 in 12		0.410	0.363	0.378	0.371
IR3503	Camo Green	783	4 in 12		0.464	0.411	0.429	0.408
IR3108	Light Gray	784	4 in 12		0.433	0.377	0.397	0.381
IR3308	Terracotta	785	4 in 12		0.473	0.416	0.443	0.425
NIR3900	Onyx	786	4 in 12		0.422	0.430	0.410	0.392

Appendix A

Richmond Exposure Site (RS05)

Painted metal, clay and concrete tile roof products with and without cool color pigments were placed on top of the steep-slope roof at Steelscape Inc.'s warehouse in Richmond, CA. Coupons of the roof products were installed in exposure rack assemblies, which are 5.5-ft high by 9-ft long, and divided into three sub-frames having respective slopes of 2-, 4- and 8-in of rise for 12-in of run (i.e., slopes of 9.5°, 18.4° and 33.7°). Each sub-frame can hold two "Sure-Grip" sub-assemblies, which are designed to have 6 rows of samples with 34-in of usable space in each row. Sample size is 3.5-in by 3.5-in. Orientation of the racks was set at 235° CCW (facing directly east represents 0° CCW), so the roof coupons faced south, south-west to receive almost full solar exposure.

Figure A.5. Exposure rack mounted on the roof of the Steelscape warehouse in Richmond, CA.

Richmond, CA Solar Reflectance Field Data

Table A.5

				Exposure Time (yrs)				
	Identifier	**Code**	**Slope**	**0.000**	**0.748**	**0.959**	**1.638**	**2.501**
	BASF PVDF Painted Metal							
Regal White	872W2	400	2 in 12	0.742	0.632	0.632	0.718	0.720
	872W2	401	4 in 12	0.742	0.633	0.633	0.716	0.720
	872W2	402	8 in 12	0.742	0.620	0.620	0.713	0.724
	815W98	403	4 in 12	0.688	0.581	0.581	0.661	0.670
Rawhide	872T6	404	2 in 12	0.569	0.492	0.492	0.546	
	872T6	405	4 in 12	0.569	0.490	0.490	0.544	
	872T6	406	8 in 12	0.568	0.484	0.484	0.544	
	836T223	407	4 in 12	0.440	0.381	0.381	0.415	0.429
Slate Blue	872B7	408	2 in 12	0.282	0.257	0.257	0.262	0.265
	872B7	409	4 in 12	0.281	0.259	0.259	0.261	0.275
	872B7	410	8 in 12	0.280	0.256	0.256	0.260	0.275
	815B49	411	4 in 12	0.172	0.172	0.172	0.161	0.174
Brick Red	872R10	412	2 in 12	0.374	0.341	0.341	0.358	0.376
	872R10	413	4 in 12	0.375	0.339	0.339	0.360	0.375
	872R10	414	8 in 12	0.373	0.340	0.340	0.357	0.375
	815R71	415	4 in 12	0.195	0.192	0.192	0.184	0.198
Charcoal Gray	872D6	416	2 in 12	0.308	0.297	0.297	0.301	0.319
	872D6	417	4 in 12	0.308	0.295	0.295	0.300	0.317
	872D6	418	8 in 12	0.308	0.294	0.294	0.299	
	815D119	419	4 in 12	0.122	0.132	0.132	0.115	0.126
Hartford Green	872G16	420	2 in 12	0.272	0.264	0.264	0.262	0.278
	872G16	421	4 in 12	0.273	0.260	0.260	0.261	0.275
	872G16	422	8 in 12	0.272	0.260	0.260	0.258	0.276
	815G37	423	4 in 12	0.088	0.106	0.106	0.084	0.094
Slate Bronze	872T3	424	2 in 12	0.262	0.252	0.252	0.254	0.269
	872T3	425	4 in 12	0.263	0.252	0.252	0.254	0.270
	872T3	426	8 in 12	0.263	0.250	0.250	0.251	0.266
	815T119	427	4 in 12	0.118	0.127	0.127	0.112	0.123
	MCA Clay Tile							
White Buff	2F44	428	2 in 12	0.630	0.585	0.585	0.585	0.583
	2F44	429	4 in 12	0.643	0.585	0.585	0.603	0.601
	2F44	430	8 in 12	0.651	0.564	0.564	0.586	0.590
Apricot Buff	CF50	431	2 in 12	0.602	0.529	0.529	0.539	0.531
	CF50	432	4 in 12	0.599	0.511	0.511	0.535	0.532
	CF50	433	8 in 12	0.607	0.549	0.549	0.566	0.564
Adobe Gray	2F71	434	2 in 12	0.424	0.395	0.395	0.397	0.404
	2F71	435	4 in 12	0.441	0.388	0.388	0.393	0.400
	2F71	436	8 in 12	0.427	0.390	0.390	0.395	0.401
Regency Blue	2F52	437	2 in 12	0.435	0.389	0.389	0.369	0.378
	2F52	438	4 in 12	0.433	0.385	0.385	0.374	0.382
	2F52	439	8 in 12	0.432	0.372	0.372	0.366	0.375
Natural Red	F40	440	2 in 12	0.459	0.408	0.408	0.411	0.418
	F40	441	4 in 12	0.458	0.419	0.419	0.427	0.433
	F40	442	8 in 12	0.461	0.428	0.428	0.428	0.434
Weathered Green	B305	443	2 in 12	0.420	0.362	0.362	0.373	0.373
	B305	444	4 in 12	0.411	0.385	0.385	0.387	0.396
	B305	445	8 in 12	0.413	0.362	0.362	0.374	0.382
Ironwood	2F19	446	2 in 12	0.269	0.258	0.258	0.245	0.259
	2F19	447	4 in 12	0.272	0.259	0.259	0.247	0.263
	2F19	448	8 in 12	0.268	NA	NA	0.249	0.265
	US Clay Tile							
Buff Blend		479	2 in 12		0.585	0.585	0.552	0.577
Bermuda Blend		480	2 in 12		0.489	0.489	0.457	0.467
	Monierlife Concrete Roof Tile							
Terra Cotta Red	6978	449	2 in 12		0.196	0.196	0.177	0.207
	6978	450	4 in 12		0.180	0.180	0.176	0.210
	6978	451	8 in 12		0.194	0.194	0.184	0.219
Hearthside	3083	452	2 in 12		0.125	0.125	0.154	0.159
	3083	453	4 in 12		0.134	0.134	0.142	0.160
	3083	454	8 in 12		0.125	0.125	0.137	0.155
Riversidepebble	3080	455	2 in 12		0.154	0.154	0.175	0.189
	3080	456	4 in 12		0.139	0.139	0.161	0.171
	3080	457	8 in 12		0.143	0.143	0.171	0.166
Ebony	5047	458	2 in 12		0.146	0.146	0.123	0.144
	5047	459	4 in 12		0.145	0.145	0.130	0.151
	5047	460	8 in 12		0.141	0.141	0.128	0.148
Lincoln Green	4087	461	2 in 12		0.157	0.157	0.165	0.193
	4087	462	4 in 12		0.171	0.171	0.174	0.206
	4087	463	8 in 12		0.161	0.161	0.163	0.192

Richmond, CA Solar Reflectance Field Data

Table A.5

				Exposure Time (yrs)				
	Identifier	Code	Slope	0.000	0.748	0.959	1.638	2.501
	Shepherd Artic Match							
Blue Artic		464	2 in 12		0.230	0.230	0.214	0.223
		465	4 in 12		0.234	0.234	0.215	0.237
		466	8 in 12		0.241	0.241	0.219	0.229
Red Artic		467	2 in 12		0.284	0.284	0.266	0.266
		468	4 in 12		0.277	0.277	0.264	0.261
		469	8 in 12		0.270	0.270	0.258	0.260
Brown Artic		470	2 in 12		0.262	0.262	0.252	0.258
		471	4 in 12		0.249	0.249	0.246	0.251
		472	8 in 12		0.247	0.247	0.253	0.251
Black Artic		473	2 in 12		0.229	0.229	0.201	0.206
		474	4 in 12		0.231	0.231	0.196	0.223
		475	8 in 12		0.238	0.238	0.214	0.219
Gray Artic		476	2 in 12		0.262	0.262	0.246	0.243
		477	4 in 12		0.259	0.259	0.252	0.252
		478	8 in 12		0.256	0.256	0.242	0.244
	American Roof Coatings							
NIR3704	Ultra Marine	481	4 in 12		0.371	0.371	0.364	0.378
IR3808	Chocolate	482	4 in 12		0.410	0.410	0.389	0.398
IR3503	Camo Green	483	4 in 12		0.463	0.463	0.438	0.451
IR3108	Light Gray	484	4 in 12		0.434	0.434	0.405	0.422
IR3308	Terracotta	485	4 in 12		0.474	0.474	0.452	0.460
NIR3900	Onyx	486	4 in 12		0.428	0.428	0.445	0.443

Appendix A

Sacramento Exposure Site (RS06)

Painted metal, clay and concrete tile roof products with and without cool color pigments were placed on top of the low-slope roof at Custom-Bilt's warehouse in Sacramento, CA. Coupons of the roof products were installed in exposure rack assemblies, which are 5.5-ft high by 9-ft long, and divided into three sub-frames having respective slopes of 2-, 4- and 8-in of rise for 12-in of run (i.e., slopes of 9.5°, 18.4° and 33.7°). Each sub-frame can hold two "Sure-Grip" sub-assemblies, which are designed to have 6 rows of samples with 34-in of usable space in each row. Sample size is 3.5-in by 3.5-in. Orientation of the racks was set at 270° CCW (facing directly east represents 0° CCW), so the roof coupons faced almost directly south to receive full solar exposure.

Figure A.6. Exposure rack mounted on the low-slope roof of Custom-Bilt Metal's warehouse in Sacramento, CA.

Sacramento, CA Solar Reflectance Field Data

Table A.6

				Exposure Time (yrs)				
	Identifier	Code	Slope	0.000	0.764	0.959	1.644	2.507
	BASF PVDF Painted Metal							
Regal White	872W2	300	1.359 in 12	0.743	0.699	0.646	0.689	0.685
	872W2	301	3.313 in 12	0.742	0.708	0.630	0.699	0.686
	872W2	302	7.122 in 12	0.744	0.706	0.659	0.698	0.688
	815W98	303	3.313 in 12	0.687	0.653	0.601	0.640	0.634
Rawhide	872T6	304	1.359 in 12	0.570	0.533	0.511	0.525	0.529
	872T6	305	3.313 in 12	0.568	0.533	0.510	0.529	0.528
	872T6	306	7.122 in 12	0.568	0.535	0.508	0.531	0.533
	836T223	307	3.313 in 12	0.439	0.410	0.403	0.401	0.408
Slate Blue	872B7	308	1.359 in 12	0.281	0.263	0.282	0.257	0.267
	872B7	309	3.313 in 12	0.282	0.264	0.281	0.256	0.271
	872B7	310	7.122 in 12	0.282	0.264	0.281	0.259	0.270
	815B49	311	3.313 in 12	0.172	0.162	0.194	0.161	0.176
Brick Red	872R10	312	1.359 in 12	0.374	0.348	0.361	0.351	0.362
	872R10	313	3.313 in 12	0.373	0.348	0.361	0.353	0.365
	872R10	314	7.122 in 12	0.374	0.350	0.357	0.354	0.369
	815R71	315	3.313 in 12	0.195	0.182	0.214	0.183	0.196
Charcoal Gray	872D6	316	1.359 in 12	0.309	0.286	0.308	0.293	0.307
	872D6	317	3.313 in 12	0.308	0.288	0.310	0.296	0.311
	872D6	318	7.122 in 12	0.308	0.289	0.308	0.297	0.311
	815D119	319	3.313 in 12	0.123	0.113	0.154	0.116	0.128
Hartford Green	872G16	320	1.359 in 12	0.272	0.253	0.279	0.257	0.270
	872G16	321	3.313 in 12	0.271	0.253	0.279	0.258	0.271
	872G16	322	7.122 in 12	0.271	0.253	0.278	0.259	0.273
	815G37	323	3.313 in 12	0.088	0.084	0.126	0.085	0.097
Slate Bronze	872T3	324	1.359 in 12	0.262	0.244	0.272	0.251	0.261
	872T3	325	3.313 in 12	0.262	0.246	0.274	0.251	0.264
	872T3	326	7.122 in 12	0.262	0.247	0.271	0.251	0.264
	815T119	327	3.313 in 12	0.118	0.111	0.138	0.111	0.123
	MCA Clay Tile							
White Buff	2F44	328	1.359 in 12	0.644	0.597	0.572	0.568	0.583
	2F44	329	3.313 in 12	0.652	0.600	0.578	0.574	0.588
	2F44	330	7.122 in 12	0.630	0.596	0.584	0.585	0.580
Apricot Buff	CF50	331	1.359 in 12	0.600	0.535	0.529	0.520	0.509
	CF50	332	3.313 in 12	0.611	0.557	0.539	0.536	0.534
	CF50	333	7.122 in 12	0.606	0.554	0.545	0.539	0.537
Adobe Gray	2F71	334	1.359 in 12	0.423	0.397	0.404	0.390	0.401
	2F71	335	3.313 in 12	0.418	0.421	0.425	0.415	0.434
	2F71	336	7.122 in 12	0.423	0.412	0.419	0.409	0.419
Regency Blue	2F52	337	1.359 in 12	0.416	0.394	0.408	0.384	0.392
	2F52	338	3.313 in 12	0.428	0.388	0.398	0.375	0.384
	2F52	339	7.122 in 12	0.413	0.397	0.408	0.387	0.398
Natural Red	F40	340	1.359 in 12	0.456	0.409	0.424	0.404	0.414
	F40	341	3.313 in 12	0.457	0.426	0.432	0.427	0.435
	F40	342	7.122 in 12	0.454	0.422	0.433	0.420	0.434
Weathered Green	B305	343	1.359 in 12	0.405	0.367	0.374	0.361	0.372
	B305	344	3.313 in 12	0.405	0.370	0.372	0.361	0.371
	B305	345	7.122 in 12	0.428	0.380	0.381	0.373	0.382
Ironwood	2F19	346	1.359 in 12	0.260	0.242	0.269	0.244	0.257
	2F19	347	3.313 in 12	0.271	0.243	0.264	0.241	0.238
	2F19	348	7.122 in 12	0.269	0.243	0.267	0.241	0.256
	US Clay Tile							
Buff Blend		379	3.313 in 11		0.562	0.567	0.546	0.401
Bermuda Blend		380	3.313 in 11		0.481	0.480	0.465	0.393
	Monierlife Concrete Roof Tile							
Terra Cotta Red	6978	349	1.359 in 12		0.184	0.213	0.183	0.207
	6978	350	3.313 in 12		0.197	0.215	0.173	0.200
	6978	351	7.122 in 12		0.196	0.205	0.174	0.199
Hearthside	3083	352	1.359 in 12		0.151	0.172	0.161	0.175
	3083	353	3.313 in 12		0.125	0.158	0.169	0.164
	3083	354	7.122 in 12		0.142	0.169	0.164	0.164
Riversidepebble	3080	355	1.359 in 12		0.126	0.143	0.140	0.167
	3080	356	3.313 in 12		0.151	0.180	0.149	0.171
	3080	357	7.122 in 12		0.160	0.176	0.161	0.170
Ebony	5047	358	1.359 in 12		0.145	0.152	0.117	0.141
	5047	359	3.313 in 12		0.136	0.156	0.159	0.148
	5047	360	7.122 in 12		0.143	0.150	0.148	0.146
Lincoln Green	4087	361	1.359 in 12		0.169	0.177	0.172	0.200
	4087	362	3.313 in 12		0.173	0.186	0.128	0.193
	4087	363	7.122 in 12		0.179	0.185	0.124	0.192

Sacramento, CA Solar Reflectance Field Data

Table A.6

				Exposure Time (yrs)				
	Identifier	Code	Slope	0.000	0.764	0.959	1.644	2.507
	Shepherd Artic Match							
Blue Artic		364	1.359 in 12		0.244	0.263	0.237	0.241
		365	3.313 in 12		0.251	0.269	0.227	0.239
		366	7.122 in 12		0.246	0.259	0.216	0.217
Red Artic		367	1.359 in 12		0.275	0.286	0.244	0.247
		368	3.313 in 12		0.288	0.298	0.255	0.264
		369	7.122 in 12		0.271	0.284	0.239	0.249
Brown Artic		370	1.359 in 12		0.256	0.278	0.239	0.250
		371	3.313 in 12		0.265	0.287	0.256	0.263
		372	7.122 in 12		0.261	0.273	0.254	
Black Artic		373	1.359 in 12		0.233	0.245	0.205	0.229
		374	3.313 in 12		0.231	0.244	0.199	0.211
		375	7.122 in 12		0.220	0.234	0.187	0.200
Gray Artic		376	1.359 in 12		0.251	0.268	0.225	0.222
		377	3.313 in 12		0.249	0.266	0.225	0.229
		378	7.122 in 12		0.269	0.284	0.248	
	American Roof Coatings							
NIR3704	Ultra Marine	381	3.313 in 12		0.392	0.386	0.386	0.401
IR3808	Chocolate	382	3.313 in 12		0.410	0.395	0.387	0.393
IR3503	Camo Green	383	3.313 in 12		0.463	0.438	0.435	0.446
IR3108	Light Gray	384	3.313 in 12		0.433	0.407	0.403	0.413
IR3308	Terracotta	385	3.313 in 12		0.473	0.452	0.448	0.456
NIR3900	Onyx	386	3.313 in 12		0.417	0.445	0.432	0.423

Appendix A

McArthur Exposure Site (RS07)

Painted metal, clay and concrete tile roof products with and without cool color pigments were placed at ground level in a fenced pasture at McArthur Farms, McArthur, CA. Coupons of the roof products were installed in exposure rack assemblies, which are 5.5-ft high by 9-ft long, and divided into three sub-frames having respective slopes of 2-, 4- and 8-in of rise for 12-in of run (i.e., slopes of 9.5°, 18.4° and 33.7°). Each sub-frame can hold two "Sure-Grip" sub-assemblies, which are designed to have 6 rows of samples with 34-in of usable space in each row. Sample size is 3.5-in by 3.5-in. Orientation of the racks was set at 0° CCW and faced directly east into the rising sun for representing exposure seen on an east facing residential roof.

Figure A.7. Exposure rack ground mounted at McArthur Farms, CA.

McArthur, CA Solar Reflectance Field Data

Table A.7

				Exposure Time (yrs)				
	Identifier	**Code**	**Slope**	**0.000**	**0.764**	**0.959**	**1.644**	**2.507**
	BASF PVDF Painted Metal							
Regal White	872W2	800	2 in 12	0.742	0.720	0.697	0.719	0.725
	872W2	801	4 in 12	0.741	0.723	0.704	0.725	0.729
	872W2	802	8 in 12	0.741	0.725	0.701	0.722	0.726
	815W98	803	4 in 12	0.690	0.665	0.658	0.667	0.667
Rawhide	872T6	804	2 in 12	0.571	0.548	0.543	0.551	
	872T6	805	4 in 12	0.570	0.546	0.544	0.547	
	872T6	806	8 in 12	0.571	0.545	0.545	0.547	
	836T223	807	4 in 12	0.440	0.420	0.426	0.416	
Slate Blue	872B7	808	2 in 12	0.282	0.271	0.277	0.265	0.280
	872B7	809	4 in 12	0.283	0.270	0.277	0.263	0.281
	872B7	810	8 in 12	0.282	0.271	0.227	0.265	0.279
	815B49	811	4 in 12	0.171	0.164	0.176	0.161	0.175
Brick Red	872R10	812	2 in 12	0.375	0.357	0.376	0.366	0.383
	872R10	813	4 in 12	0.375	0.357	0.375	0.364	0.383
	872R10	814	8 in 12	0.376	0.359	0.376	0.366	0.383
	815R71	815	4 in 12	0.195	0.186	0.201	0.184	.277- bird poop
Charcoal Gray	872D6	816	2 in 12	0.308	0.294	0.316	0.304	0.317
	872D6	817	4 in 12	0.308	0.294	0.317	0.302	0.320
	872D6	818	8 in 12	0.307	0.294	0.316	0.304	0.320
	815D119	819	4 in 12	0.122	0.119	0.133	0.116	0.128
Hartford Green	872G16	820	2 in 12	0.272	0.258	0.281	0.264	0.280
	872G16	821	4 in 12	0.272	0.256	0.279	0.261	0.278
	872G16	822	8 in 12	0.270	0.259	0.279	0.266	0.280
	815G37	823	4 in 12	0.088	0.087	0.099	0.084	0.096
Slate Bronze	872T3	824	2 in 12	0.262	0.251	0.268	0.256	0.270
	872T3	825	4 in 12	0.263	0.251	0.270	0.255	0.272
	872T3	826	8 in 12	0.262	0.251	0.269	0.255	0.270
	815T119	827	4 in 12	0.117	0.115	0.128	0.112	0.125
	MCA Clay Tile							
White Buff	2F44	828	2 in 12	0.630	0.612	0.597	0.606	0.608
	2F44	829	4 in 12	0.632	0.612	0.614	0.611	0.617
	2F44	830	8 in 12	0.643	0.619	0.614	0.619	0.626
Apricot Buff	CF50	831	2 in 12	0.617	0.621	0.612	0.615	0.618
	CF50	832	4 in 12	0.597	0.567	0.568	0.567	0.577
	CF50	833	8 in 12	0.607	0.580	0.582	0.582	0.590
Adobe Gray	2F71	834	2 in 12	0.446	0.417	0.430	0.424	0.433
	2F71	835	4 in 12	0.448	0.403	0.419	0.407	0.423
	2F71	836	8 in 12	0.436	0.425	0.441	0.430	0.449
				.				
Regency Blue	2F52	837	2 in 12	0.424	0.413	0.418	0.410	0.418
	2F52	838	4 in 12	0.417	0.415	0.418	0.414	0.425
	2F52	839	8 in 12	0.420	0.400	0.406	0.400	0.405
Natural Red	F40	840	2 in 12	0.457	0.430	0.435	0.427	0.445
	F40	841	4 in 12	0.467	0.420	0.429	0.421	0.441
	F40	842	8 in 12	0.459	0.442	0.451	0.442	0.460
Weathered Green	B305	843	2 in 12	0.405	0.378	0.387	0.376	0.398
	B305	844	4 in 12	0.402	0.396	0.418	0.397	0.413
	B305	845	8 in 12	0.408	0.387	0.399	0.391	0.408
Ironwood	2F19	846	2 in 12	0.261	0.250	0.269	0.253	0.265
	2F19	847	4 in 12	0.263	0.247	0.265	0.251	0.274
	2F19	848	8 in 12	0.263	0.249	0.265	0.250	0.268
	US Clay Tile							
Buff Blend		879	2 in 12		0.578	0.576	0.577	0.563
Bermuda Blend		880	2 in 12		0.493	0.486	0.490	0.496
	Monierlife Concrete Roof Tile							
Terra Cotta Red	6978	849	2 in 12		0.186	0.192	0.176	0.204
	6978	850	4 in 12		0.196	0.200	0.200	0.204
	6978	851	8 in 12		0.186	0.194	0.182	0.213
Hearthside	3083	852	2 in 12		0.140	0.153	0.157	0.175
	3083	853	4 in 12		0.131	0.164	0.146	0.179
	3083	854	8 in 12		0.136	0.150	0.160	0.168
Riversidepebble	3080	855	2 in 12		0.136	0.149	0.148	0.138
	3080	856	4 in 12		0.135	0.139	0.146	0.160
	3080	857	8 in 12		0.143	0.152	0.145	0.155
Ebony	5047	858	2 in 12		0.137	0.145	0.125	0.157
	5047	859	4 in 12		0.140	0.135	0.115	0.133
	5047	860	8 in 12		0.137	0.134	0.117	0.148
Lincoln Green	4087	861	2 in 12		0.171	0.181	0.165	0.193
	4087	862	4 in 12		0.156	0.155	0.155	0.165
	4087	863	8 in 12		0.162	0.161	0.160	0.185

McArthur, CA Solar Reflectance Field Data

Table A.7

				Exposure Time (yrs)				
	Identifier	Code	Slope	0.000	0.764	0.959	1.644	2.507
	Shepherd Artic Match							
Blue Artic		864	2 in 12		0.240	0.258	0.229	0.245
		865	4 in 12		0.236	0.249	0.227	0.239
		866	8 in 12		0.240	0.243	0.227	0.228
Red Artic		867	2 in 12		0.259	0.274	0.247	0.254
		868	4 in 12		0.332	0.320	0.295	0.300
		869	8 in 12		0.267	0.260	0.263	0.266
Brown Artic		870	2 in 12		0.260	0.273	0.254	0.259
		871	4 in 12		0.250	0.273	0.249	0.260
		872	8 in 12		0.256	0.277	0.258	0.265
Black Artic		873	2 in 12		0.230	0.235	0.207	0.209
		874	4 in 12		0.240	0.239	0.208	0.224
		875	8 in 12		0.240	0.239	0.201	0.219
Gray Artic		876	2 in 12		0.269	0.285	0.252	0.230
		877	4 in 12		0.273	0.285	0.256	0.259
		878	8 in 12		0.263	0.282	0.258	0.269
	American Roof Coatings							
NIR3704	Ultra Marine	881	4 in 12		0.391	0.392	0.389	0.401
IR3808	Chocolate	882	4 in 12		0.410	0.410	0.397	0.411
IR3503	Camo Green	883	4 in 12		0.466	0.466	0.451	0.467
IR3108	Light Gray	884	4 in 12		0.434	0.429	0.412	0.426
IR3308	Terracotta	885	4 in 12		0.474	0.477	0.464	0.478
NIR3900	Onyx	886	4 in 12		0.436	0.487	0.464	0.466

Appendix B
Additional notes on soil optical properties

In support of the ORNL/LBNL report to CEC (Task 2.6.2), we show how to compute the absorptance and reflectance of a soil layer from measurements of solar reflectance on light and dark samples. It was shown in the report that winter rains cleaned much of the accumulated dust on PVDF films. Here we make that observation more quantitative. Of the deposits remaining after winter rains, the absorptance and reflectance are positively correlated with measured iron concentrations.

Suppose a substrate has a clean reflectance denoted *Ro*, which is coated with a thin soil layer with absorptance *a* and reflectance *r*. In view of the assumption that the layer is thin, we take both *a* and *r* as small compared to unity. Then, it is not difficult to show that the change in reflectance (*R* - *Ro*) of the soiled substrate is given, to first order in *r* and *a*, by

$$R - Ro = -2Ro\,a + (1 - Ro)2r. \qquad (1)$$

[This equation was derived by summing the different ways a photon can be reflected as $(1\text{-}a\text{-}r)^2\,Ro$ {transmitted twice through the soil layer and reflected from the substrate} plus *r* {reflection from the soil layer}, plus $(1\text{-}a\text{-}r)^2\,r\,Ro^2$ {transmitted twice, reflected once from the underside of the soil layer, and twice from the substrate}]. Thus soil absorptance reduces *R* and soil reflectance increases *R*. Here we can also see that *a* will be less important if *Ro* is small and *r* will be less important if *Ro* is close to unity. Stated another way, for highly reflective materials (*Ro* close to 1), we expect a decline in reflectance due to the soil absorptance *a*. For very dark materials, we expect an increase in reflectance due to the soil reflectance *r*.

The soil parameters *a* and *r* can be determined by fitting if reflectance change measurements are available for two or more substrates with different *Ro*. For fitting purposes it is useful to divide Eq. (1) by *Ro*:

$$(R - Ro)/Ro = -2a + [(1 - Ro)^2/Ro]\,r. \qquad (2)$$

Then a plot of (*R* – *Ro*) /*Ro* versus *Ro* produces a horizontal line at height –2 *a* if *r* is negligible, and increases at decreasing *Ro* if *r* is not negligible. Figure B1 shows an example of the fitting procedure, for Shafter at 1 year. The data are taken from Appendix A of report 2.6.2, using the PVDF samples. The slope chosen is that for which there are both cool and standard samples. The open circles are the fitted curve. A color photograph of a Shafter sample at 1 year is also included in report 2.6.2. Figure B2 shows similar fits for the other 6 sites at 1 year. Figure B3 shows data for Shafter after 1.6 years. At this point it was spring in California and much of the soil deposits have been removed by rain. In this figure the fitted curve was forced to pass through the highest reflectance data point (white) at *Ro* = 0.74 and the non-selective gray at *Ro* = 0.123, because some of the scatter in the data points might be due to spectrally selective interaction between the various substrates and the spectral properties of the soil. Also, in the presence of data scatter, it is desirable to use substrates with widely different *Ro*.

Figure 4 shows similar plots for the other 6 sites. Despite the scatter, in all cases we obtain a non-zero value for *a*. In most cases we obtain a value for *r*, but it is sometimes not distinguishable from zero.

Appendix B
Additional notes on soil optical properties

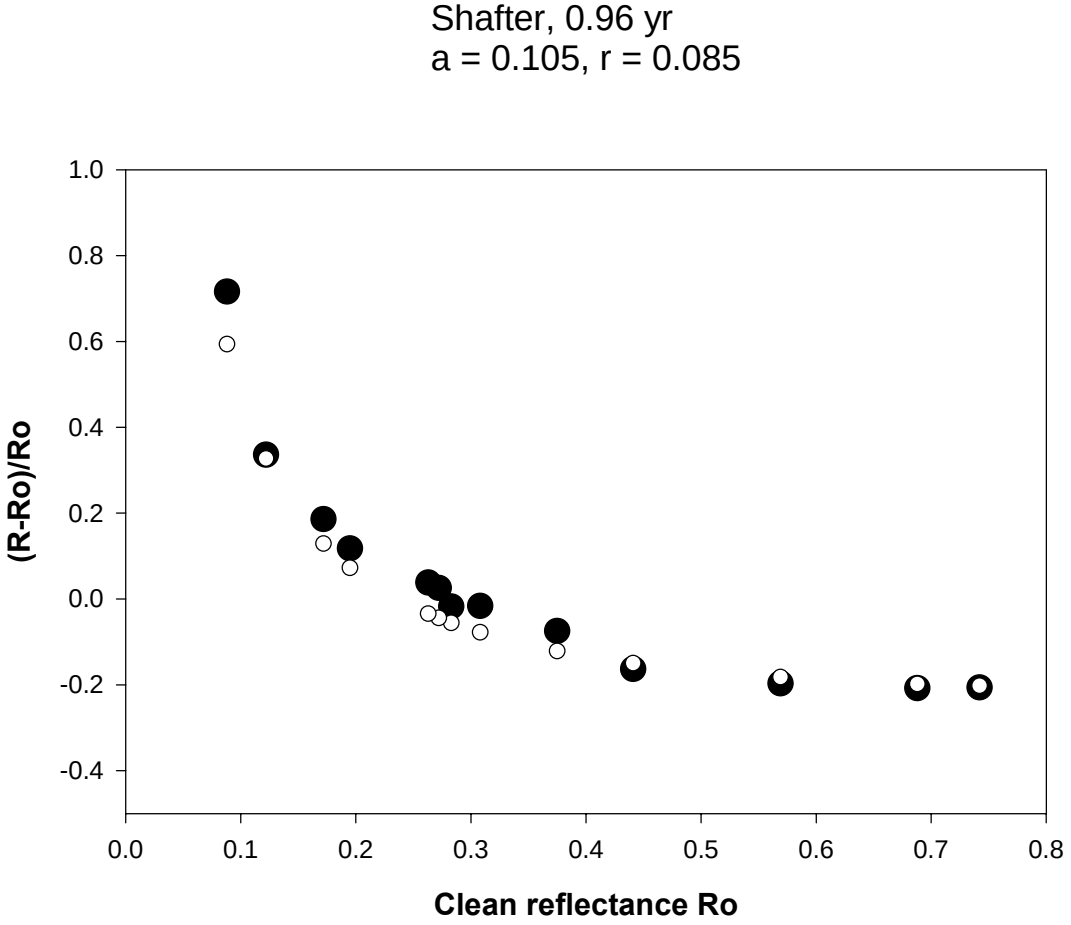

Fig. B1. Measured (solid circles) and fitted (open circles) changes in reflectance due to sample soiling. High reflectance samples lose reflectance; low-reflectance samples gain reflectance.

The results of the curve fitting exercise are collected in Table B1. Judging by the absorptances, the amount of material remaining at 1.6 years is only ½ to ⅛ of that present at 1 year. Thus the weathering, presumably due to dew and rain transport, significantly cleaned the substrates. Note that already even at 1 year, the photograph of the Shafter sample in Fig. B4 of report 2.6.2 shows transport of soil along the surface of the sample to the lower edge. Thus the weathering process significantly alters the original dry atmospheric deposition. Note that the *r*-values were reduced even more than *a*-values at 1.6 years, compared to 1 year. This means that the weathering process not only reduced the quantity of soil originally deposited, but that it altered the composition as well. Of course water-soluble components are expected to be transported by rain, but small and low-density particles are likely to be transported as well. Remaining particles are likely to be larger in size, higher in density, and/or able to adhere to the substrate.

Finally, Table B2 shows the measured concentrations of iron, organic carbon, and elemental carbon at 1.6 years. Plotting *a*- and *r*-values against iron concentration in Fig. B5, we find that higher values of these parameters are associated with higher iron concentrations. The statistical R^2 values are 0.48 for *a* and 0.38 for *r*. Corresponding values for organic carbon (0.03 for *a*) and elemental carbon (0.01 for *a*) were quite low.

Appendix B
Additional notes on soil optical properties

The tentative picture that emerges is that iron-containing mineral dust tends to remain on the Teflon-like PVDF surfaces washed by rain. Concentrations of iron were as large as about 70 mg/m^2. Iron in the ferric 3+ valence state is associated with strong absorption in the short wavelength portion of the solar spectrum (wavelength < 550 nm), as in the case of small hematite particles where the absorption strength is 4 m^2/g. Multiplying these two figures we obtain a crude estimate of 0.28 for short wavelength absorptance. The short wavelength part of the solar spectrum of interest here contains about ¼ of the total solar flux. Thus we estimate that the solar average absorptance due to 70 mg/m^2 of iron could be about 0.07. This number compares well with the ~ 0.05 absorptance at the sites with the highest iron concentration. This rough agreement could be an accident, but at least our picture is consistent.

Table B1. Soil absorptance and reflectance at 1 year, and at 1.6 years. The 1 year data were at the end of the dry summer period, while the 1.6 year data were obtained in the spring, after winter rainfall.

Site	**1 year**	**1 year**	**1 yr**	**1.6 years**	**1.6 years**	**1.6 yr**
	absorptance ***a***	**reflectance** ***r***	***r/a***	**absorptance** ***a***	**Reflectance** ***r***	***r/a***
El Centro	0.10	0.13	1.3	0.012	0.009	0.8
Corona	0.090	0.085	0.9	0.048	0.013	0.3
Colton	0.14	0.15	1.1	0.045	0.008	0.2
Shafter	0.105	0.085	0.8	0.04	0.005	0.1
Richmond	0.075	0.036	0.5	0.025	< 0.003	< 0.1
Sacramento	0.060	0.058	1.0	0.03	< 0.003	< 0.1
McArthur	0.025	0.021	0.8	0.022	< 0.003	< 0.2

Table 2. Concentrations of three substances that could be associated with soil absorptance and reflectance. Iron has a significant correlation (see Fig. B5).

Site	**Exposure Time (1.6 years)**		
	Iron (mg/m^2)	Organic C **(mg/m^2)**	Elemental C **(mg/m^2)**
El Centro	33	8.3	0.2
Corona	68	5.5	0.2
Colton	67	6.1	0.2
Shafter	32	5.6	0.4
Richmond	44	11	1.3
Sacramento	42	4.5	0.2
McArthur	5	1.3	~ 0.02

Appendix B
Additional notes on soil optical properties

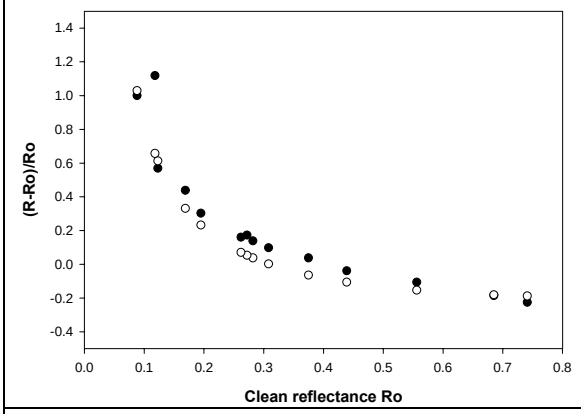

Fig. B2a

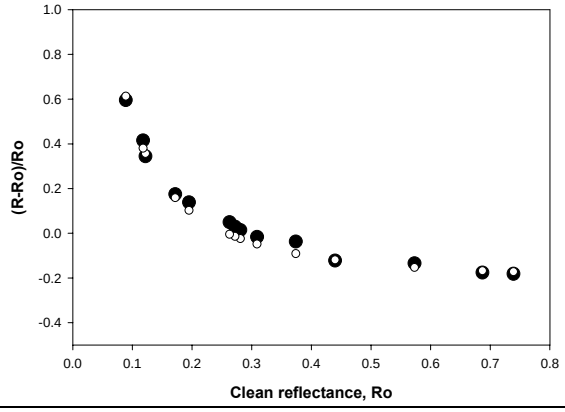

Fig. B2b

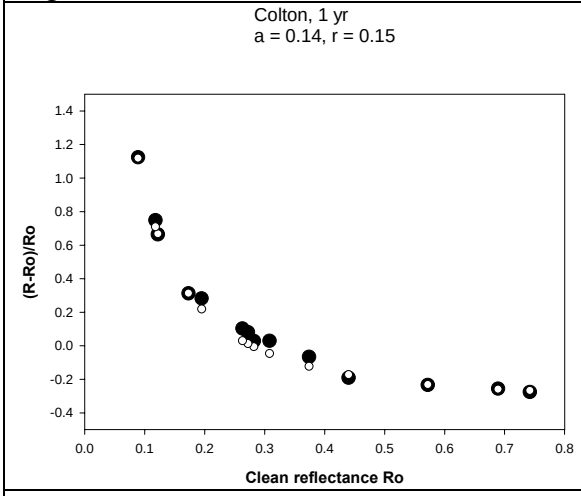

Fig. B2c

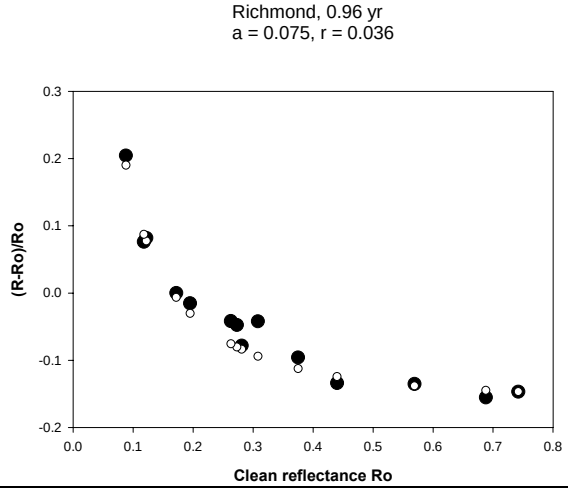

Fig. B2d

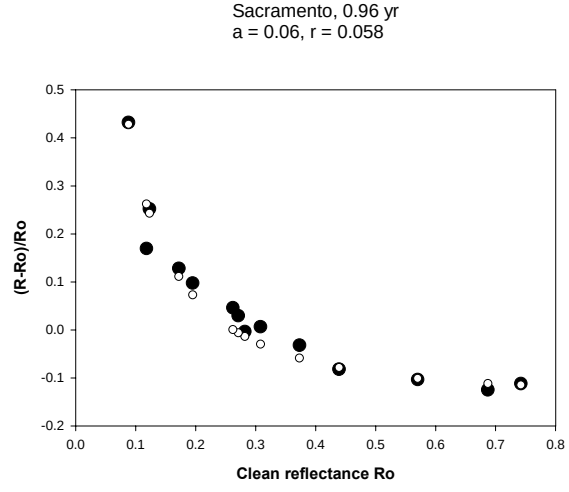

Fig. B2e

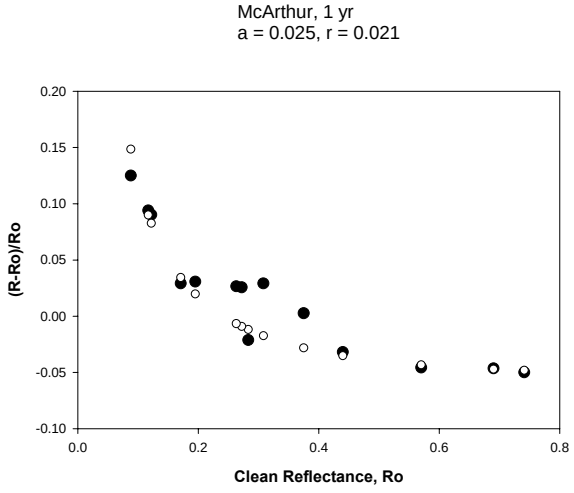

Fig. B2f

Appendix B
Additional notes on soil optical properties

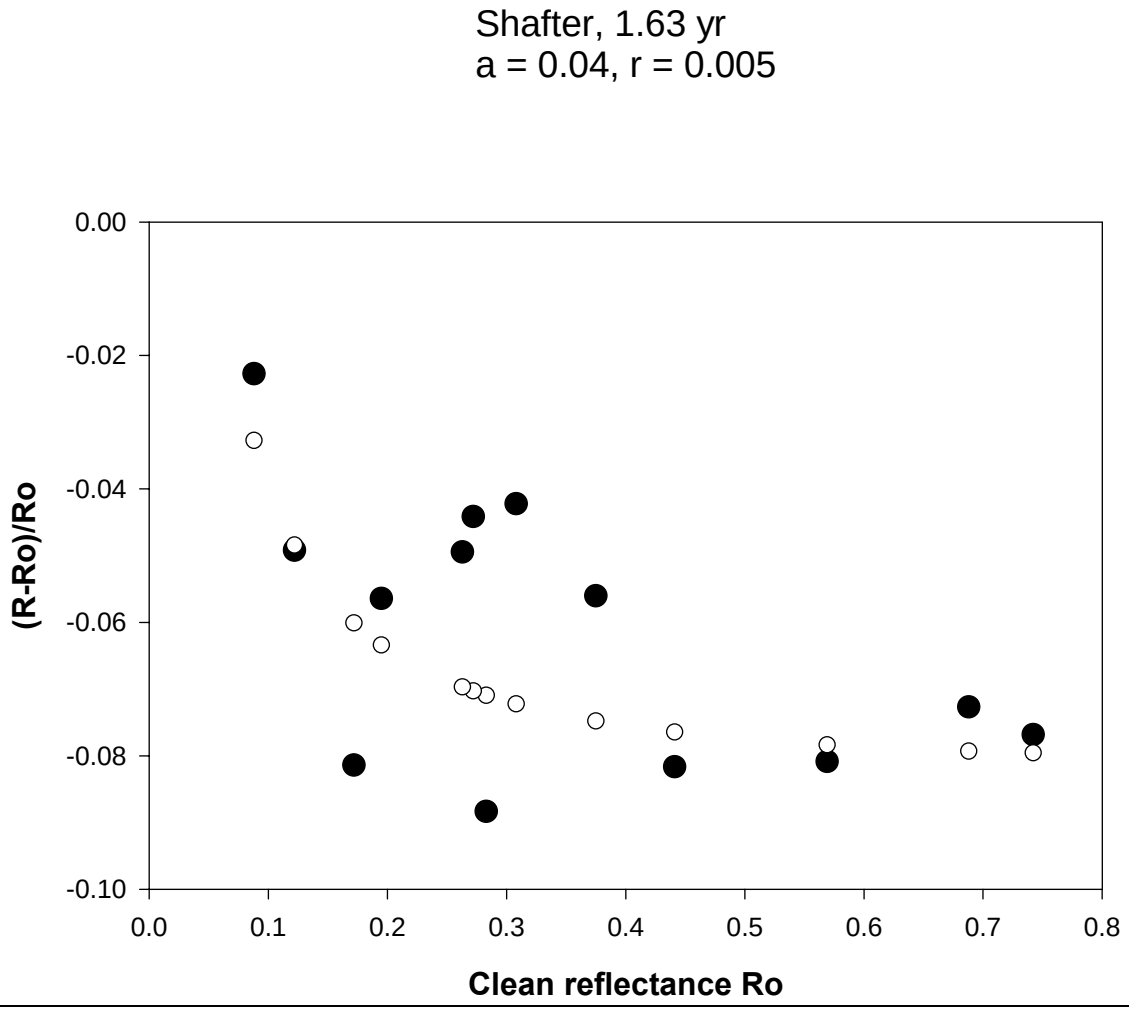

Figure B3. Data for Shafter as in Fig.1, but at 1.6 years rather than 1 year. Smaller values for a and r indicate that less dust is present.

Appendix B
Additional notes on soil optical properties

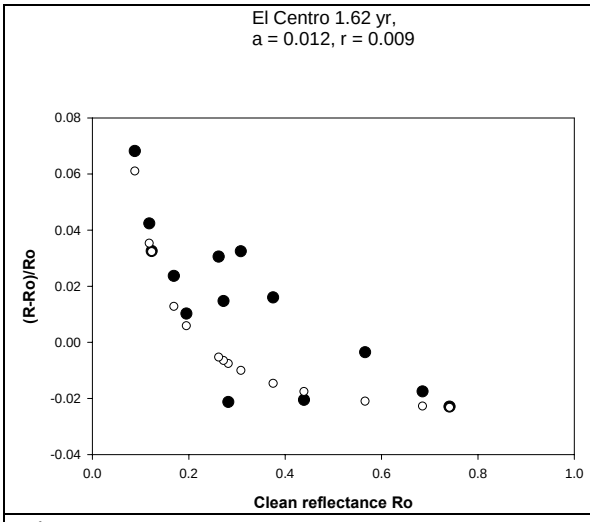

Fig. B4a

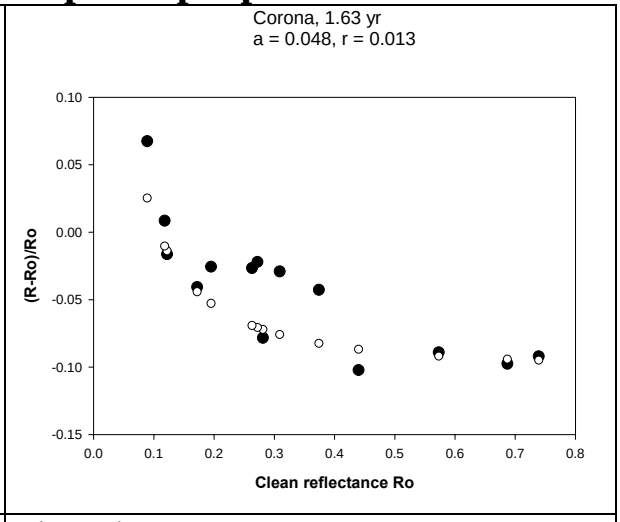

Fig. B4b

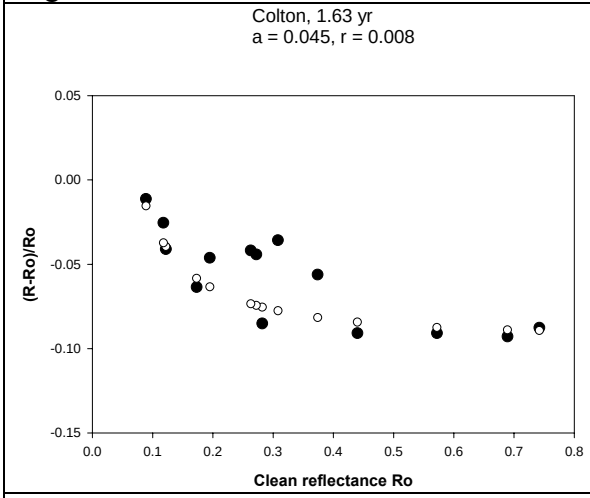

Fig. B4c

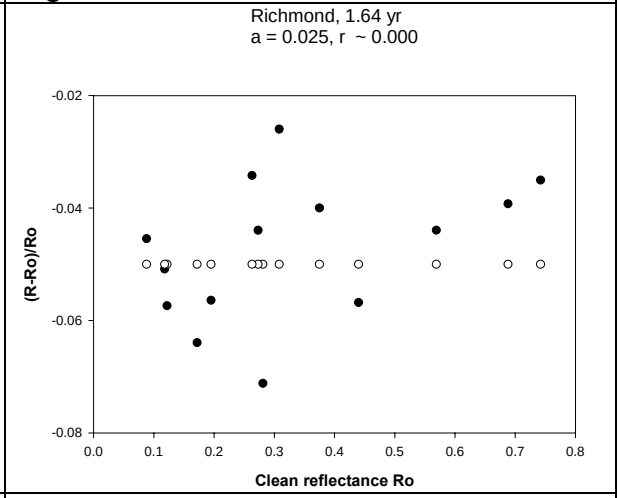

Fig. B4d

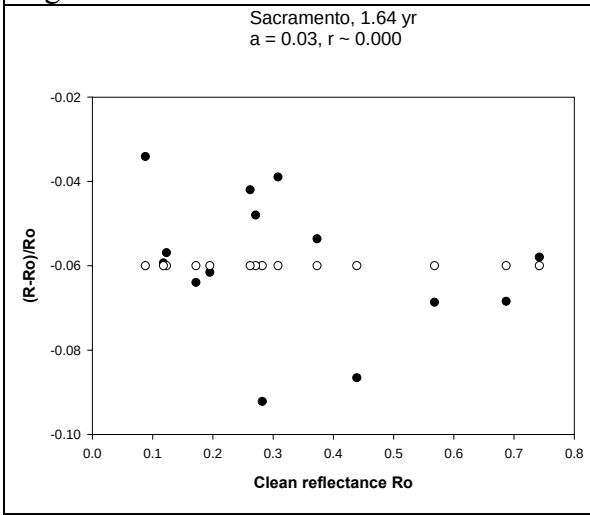

Fig. B4e

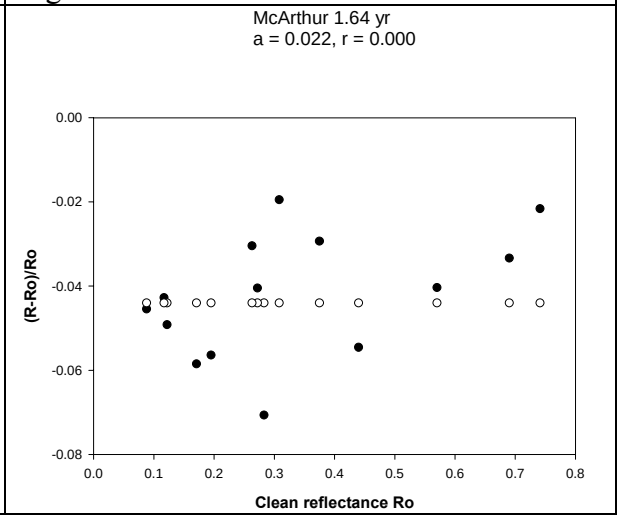

Fig. B4f

Appendix B
Additional notes on soil optical properties

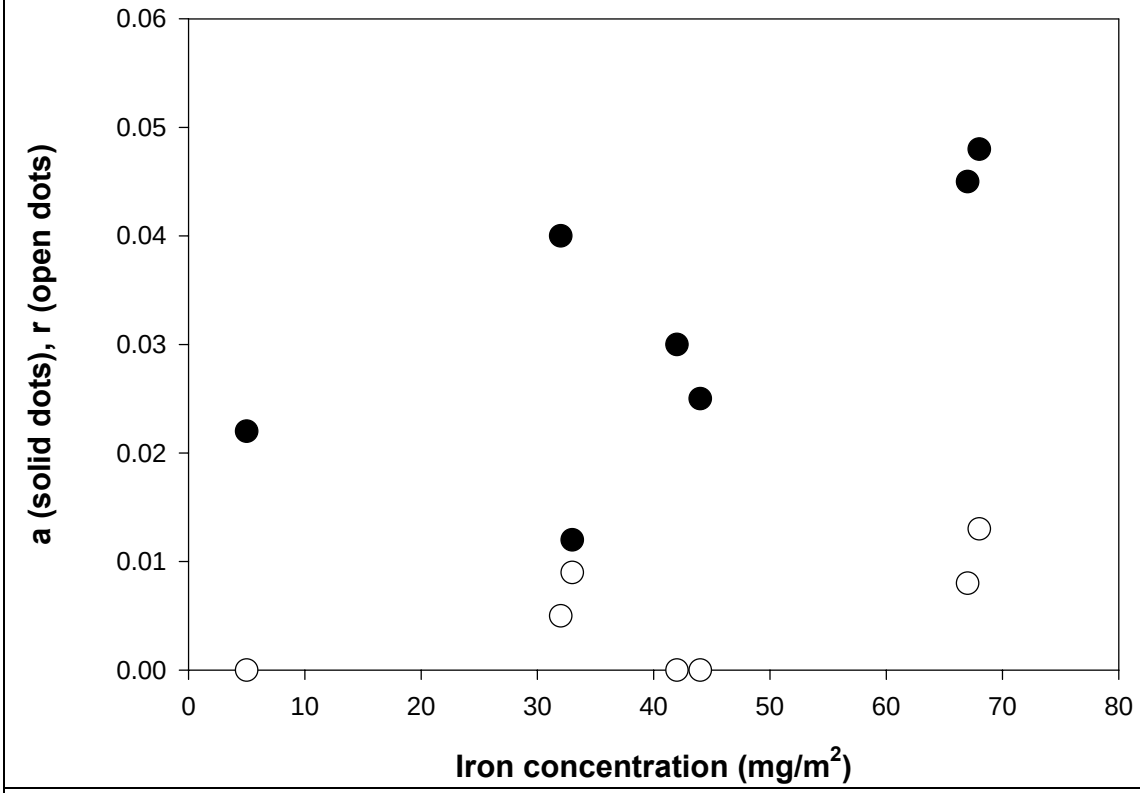

Fig. 5. A plot of data highlighted in Table 1. There are positive correlations of both soil absorptance *a* and soil reflectance *r* with iron concentration.